AGARD-AG-162-Part III

ARD
RESEARCH & DEVELOPMENT
LY SUR SEINE FRANCE

AGARDograph No. 162

on

Acoustic Fatigue Design Data

Part III

by

A.G.R.Thomson and R.F.Lambert

H ATLANTIC TREATY ORGANIZATION

NORTH ATLANTIC TREATY ORGANIZATION

ADVISORY GROUP FOR AEROSPACE RESEARCH AND DEVELOPMENT

(ORGANISATION DU TRAITE DE L'ATLANTIQUE NORD)

AGARDograph 162

ACOUSTIC FATIGUE DESIGN DATA

Part III

by

A.G.R.Thomson and R.F.Lambert

Engineering Sciences Data Unit Ltd
London, UK

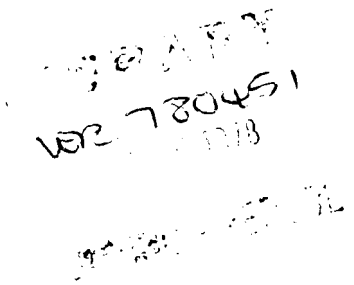

This AGARDograph was sponsored by the Structures and Materials Panel of AGARD

THE MISSION OF AGARD

The mission of AGARD is to bring together the leading personalities of the NATO nations in the fields of science and technology relating to aerospace for the following purposes:

- Exchanging of scientific and technical information;
- Continuously stimulating advances in the aerospace sciences relevant to strengthening the common defence posture;
- Improving the co-operation among member nations in aerospace research and development;
- Providing scientific and technical advice and assistance to the North Atlantic Military Committee in the field of aerospace research and development;
- Rendering scientific and technical assistance, as requested, to other NATO bodies and to member nations in connection with research and development problems in the aerospace field;
- Providing assistance to member nations for the purpose of increasing their scientific and technical potential;
- Recommending effective ways for the member nations to use their research and development capabilities for the common benefit of the NATO community.

The highest authority within AGARD is the National Delegates Board consisting of officially appointed senior representatives from each member nation. The mission of AGARD is carried out through the Panels which are composed of experts appointed by the National Delegates, the Consultant and Exchange Program and the Aerospace Applications Studies Program. The results of AGARD work are reported to the member nations and the NATO Authorities through the AGARD series of publications of which this is one.

Participation in AGARD activities is by invitation only and is normally limited to citizens of the NATO nations.

Published December 1973

620.178.3:539.431:624.07

Printed by Technical Editing and Reproduction Ltd
Harford House, 7–9 Charlotte St. London. W1P 1HD

PREFACE

This volume, the third part of a series giving data for design against acoustic fatigue, has been prepared in order to draw together the results of research in acoustic fatigue and to present them in a form directly useable in aerospace design. Future work in this series will deal with endurance of titanium alloy structures under simulated acoustic loading, near field compressor noise estimation, stress response of box and control surface structures, structural damping and stress response of skin-stringer panels with stringers of relatively low flexural stiffness.

The AGARD Structures and Materials Panel has for many years been active in encouraging and coordinating the work that has been necessary to make this collection of design data possible and after agreeing on procedures for the acquisition, analysis and interpretation of the requisite data, work on this series of design data sheets was initiated in 1970.

The overall management of the project has been conducted by the Working Group on Acoustic Fatigue of the AGARD Structures and Materials Panel, and the project has been financed through a collective fund established by the Nations collaborating in the project, namely Canada, France, Germany, Italy, UK and US. National Coordinators appointed by each country have provided the basic data, liaised with the sources of the data, and provided constructive comment on draft data sheets. These Coordinators are Dr G.M.Lindberg (Canada), Mr R.Loubet (France), Mr G.Bayerdörfer (Germany), Gen.A.Griselli (Italy), Mr N.A.Townsend (UK), Mr A.W.Kolb (US) and Mr F.F.Rudder (US). Staff of the Engineering Sciences Data Unit Ltd, London, have analysed the basic data and prepared and edited the resultant data sheets with invaluable guidance and advice from the National Coordinators and from the Acoustic Fatigue Panel of the Royal Aeronautical Society which has the following constitution: Professor B.L.Clarkson (Chairman), Mr D.C.G.Eaton, Mr J.A.Hay, Mr W.T.Kirkby, Mr M.J.T.Smith and Mr N.A.Townsend. The members of staff of the Engineering Sciences Data Unit concerned with the preparation of the data sheets in this volume are: Mr A.G.R.Thomson (Executive, Environmental Projects), Dr G.Sen Gupta and Mr R.F.Lambert (Environmental Projects Group).

Data sheets based on this AGARDograph will subsequently be issued in the Fatigue Series of Engineering Sciences Data issued by ESDU Ltd, where additions and amendments will be made to maintain their current applicability.

A.H.Hall
Chairman,
Working Group on Acoustic Fatigue
Structures and Materials Panel

CONTENTS

Section 1

ENDURANCE OF TITANIUM AND TITANIUM ALLOY STRUCTURAL ELEMENTS SUBJECTED TO SIMULATED ACOUSTIC LOADING

1.1 Notation

S_{rms}	root mean square value of stress at a reference position	N/m^2	lbf/in^2
N_r	equivalent endurance, taken as half the number of zero crossings of the stress-time function before failure	cycles	cycles

1.2 Notes

This Section gives the results of fatigue tests on titanium alloy specimens, typical of aircraft structural elements, excited by narrow-band loading of random amplitude with zero mean load to simulate stress response to acoustic loading.

The plain specimens, illustrated in Figure 1.1a, are representative of sheet material away from the effects of attachments. The built-up specimens, illustrated in Figures 1.1b to 1.1e represent conditions in sheet material attached without jointing compound to stiffeners, where adjacent plates are vibrating in phase.

In Figures 1.2 to 1.5, S_{rms} is plotted against N_r for test results grouped according to the type of structural element, material and method of attachment as shown in Table 1.1. A straight line fitted by the least squares method and bands enclosing approximately 95 per cent of the data, (two standard deviations either side of the mean) have been given for guidance; they should not be used directly for estimating life because due account must be taken of scatter. Figure 1.6 shows the relative endurances for the different groups. Extrapolation of the mean lines beyond the limits indicated on Figure 1.6, where few data are available, is expected to lead to an underestimate of endurance. Data from similar tests under constant amplitude loading indicate that, for titanium alloys, the S-N curve tends to level off above 10^7 cycles.

The reference position for S_{rms} is taken as a point on the failure line away from the effects of stress concentration or fretting at fastenings; the test points plotted represent either mean stresses over the areas covered by monitoring strain gauges affixed across the failure line away from fastenings, or stresses at that position estimated after calibration from strain monitors located elsewhere. When using this Section to estimate a life using a root mean square stress level obtained from Reference 1.4.5, it is recommended that the calculated value of stress at the rivet line should be assumed to be the same as the stress at the failure line. In practice the failure position is sufficiently close to the rivet line for this approximation to be within the range of accuracy of the simple theory used for stress prediction in Reference 1.4.5.

Details of the test methods and specimens are given in appendices as listed below.

Appendix 1A.1 - Tests on plain specimens
Appendix 1A.2 - Tests on fastened-skin specimens
Appendix 1A.3 - Description of materials

Typical failure locations are shown on Figure 1.1.

The loading simulated for the fastened-skin specimens is only that for modes where adjacent panels are in phase. Care should be taken in using the data for modes involving twisting of the stiffeners.

1.3 Interpretation Of The Results

1.3.1 Effect of method of attachment

Skin specimens attached to stiffeners by mushroom-headed rivets showed significantly greater endurance and less scatter than resistance spot-welded specimens. The resistance spot-welded specimens in turn showed slightly greater endurance and considerably less scatter than gas tungsten-arc spot-welded* specimens. The latter process therefore requires further development before it can be used with confidence for titanium structures in a high noise environment.

---

* The gas tungsten-arc spot welding process is described in Reference 1.4.4.

1.3.2 Effect of material specification and thickness

The available data for different materials are not directly comparable because of differences in specimen configuration and thickness. The large differences between the results for Ti-2Cu (Aged) (Figures 1.3 and 1.4) and C.P. Ti (Figure 1.5) are thought to be due to the effects of skin thickness on spot-weld performance rather than to the difference in materials.

1.3.3 Effect of heat treatment and grain direction

The tests on the Ti-2Cu material show that for this material a substantial increase in endurance is obtained by spot welding before, rather than after, ageing. For these specimens slightly greater endurance was obtained for spot welds stressed in a transverse rather than a longitudinal grain direction but the difference might not be significant.

1.3.4 Effect of test frequency

The mean response frequency for each type of test specimen is indicated in Figures 1.2 to 1.4. The range of frequencies is too small for any effects to be identified.

1.3.5 Effect of elevated temperature

A limited number of tests on Ti-2Cu (Aged) specimens was carried out at 250°C. These indicate that temperatures up to 250°C have little effect on the endurance of this material.

1.3.6 Data for plain specimens

Tests on the plain specimens, under constant amplitude loading, showed a very marked discontinuity in the S-N curve at alternating stresses of about 450 MN/m^2 (65 000 lbf/in^2). The increased scatter of the test results at r.m.s. stresses of about 250 MN/m^2 (35 000 lbf/in^2) in Figure 1.2 is believed to be associated with this discontinuity.

1.4 Derivation and References

Derivation

1.4.1 Cummins, R.J. Eaton, D.C.G. — Unpublished work by British Aircraft Corporation, May 1969.

1.4.2 Artusio, G. et al — Unpublished work by Fiat, January 1971.

1.4.3 Cummins, R.J. Eaton, D.C.G. — Unpublished work by British Aircraft Corporation, January 1971.

References

1.4.4 - — Welding Handbook, Part 2, welding processes - gas, arc and resistance. 27 20/21 5th Ed. American Welding Society, 1964.

1.4.5 Thomson, A.G.R. Lambert, R.F. — Acoustic fatigue design data, Part 2, Section 1, AGARD-AG-162-Part 2, 1972.

TABLE 1.1

SUMMARY OF DATA PRESENTED

Figure No.	Type of Element	Material	Number of Attachment Rows	Attachment Type	Thickness		Response Frequency (Hz)
					mm	in	
1.2	Plain	Ti-6Al 4V (Ann)	-	-	1.52	(0.06)	300
1.3	Riveted skin	Ti-2Cu(Aged)	1	c's'k Monel rivet	(0.71)	0.028	260
			2	m/h Monel rivet	(0.71)	0.028	160
1.4	Welded skin		1	resistance spot weld	(0.71)	0.028	250
1.5	Welded skin	C.P.Ti	2	resistance spot weld	(0.41)	0.016	190
			2	gas tungsten-arc spot weld	(0.41)	0.016	180
			1		(0.41)	0.016	175
1.6	ASSEMBLAGE OF DATA PLOTTED ON FIGURES 1.2 TO 1.5						

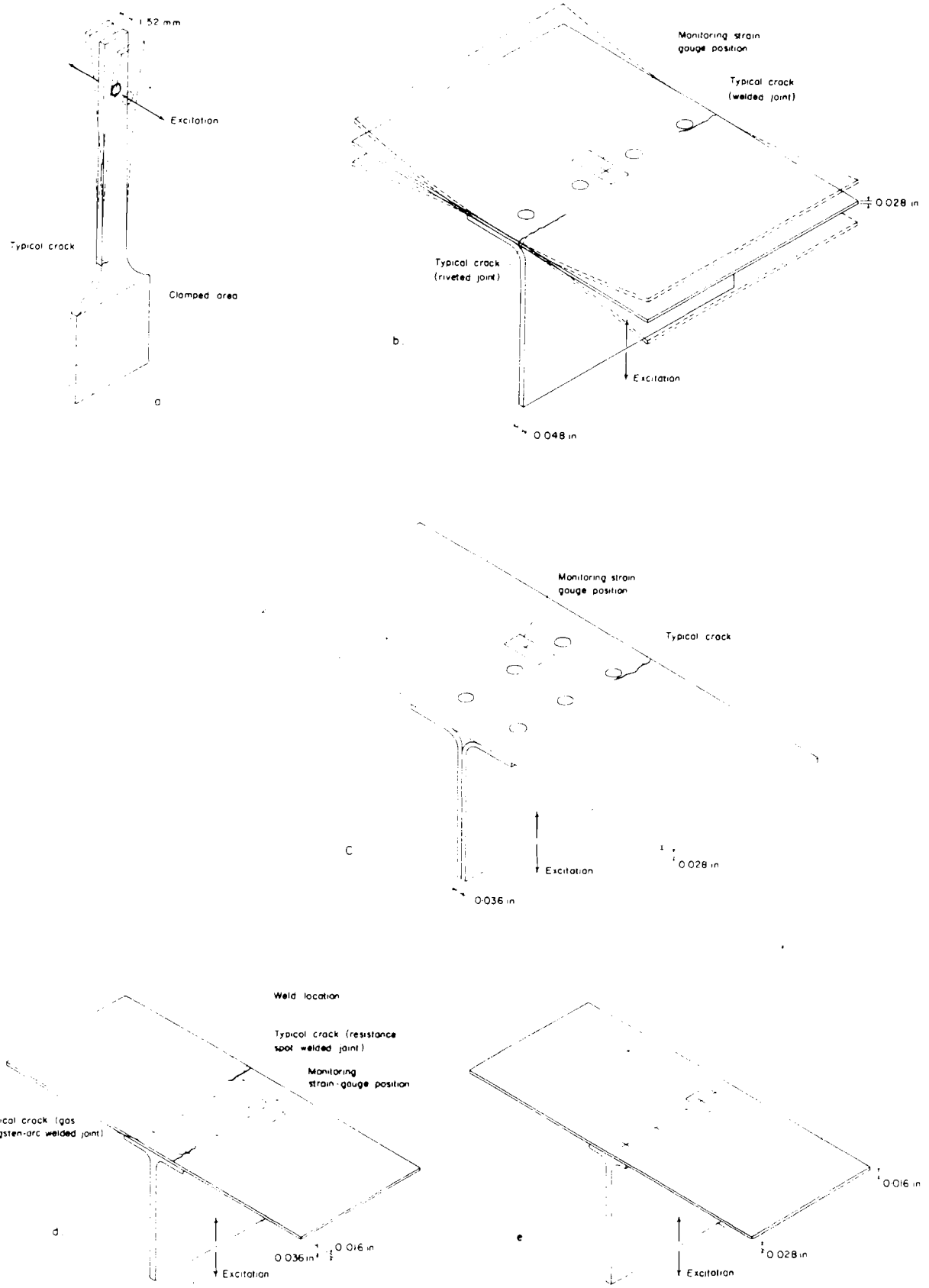
1.52 mm
Excitation
Typical crack
Clamped area
a
Monitoring strain gauge position
Typical crack (welded joint)
0.028 in
Typical crack (riveted joint)
b
Excitation
0.048 in
Monitoring strain gauge position
Typical crack
C
Excitation
0.028 in
0.036 in
Weld location
Typical crack (resistance spot welded joint)
Monitoring strain-gauge position
Typical crack (gas tungsten-arc welded joint)
d
0.036 in
0.016 in
Excitation
e
0.016 in
0.028 in
Excitation

FIGURE 1.1

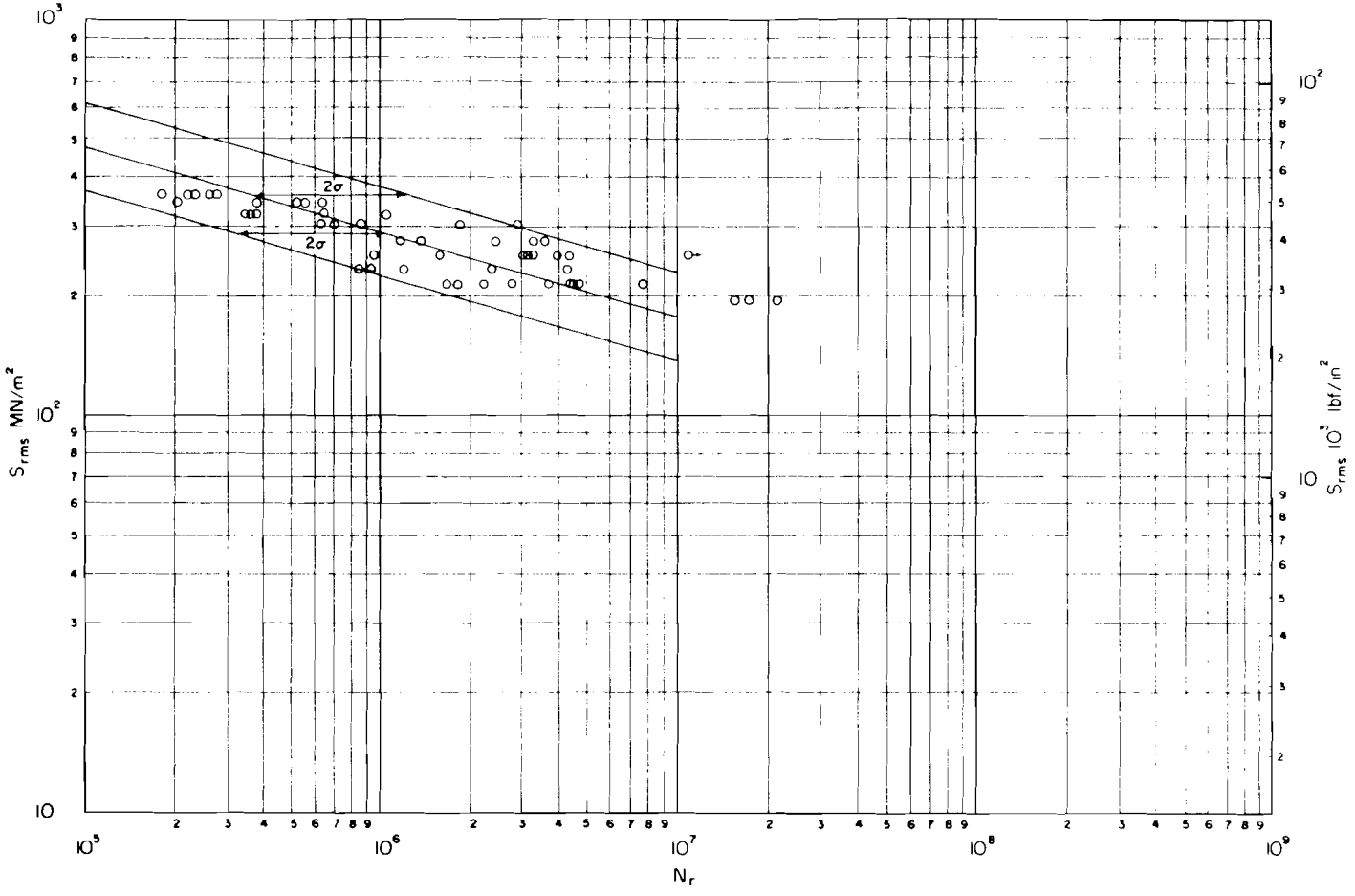

FIGURE 12 S-N DATA FOR PLAIN SPECIMENS IN Ti-6Al 4V (ANNEALED)

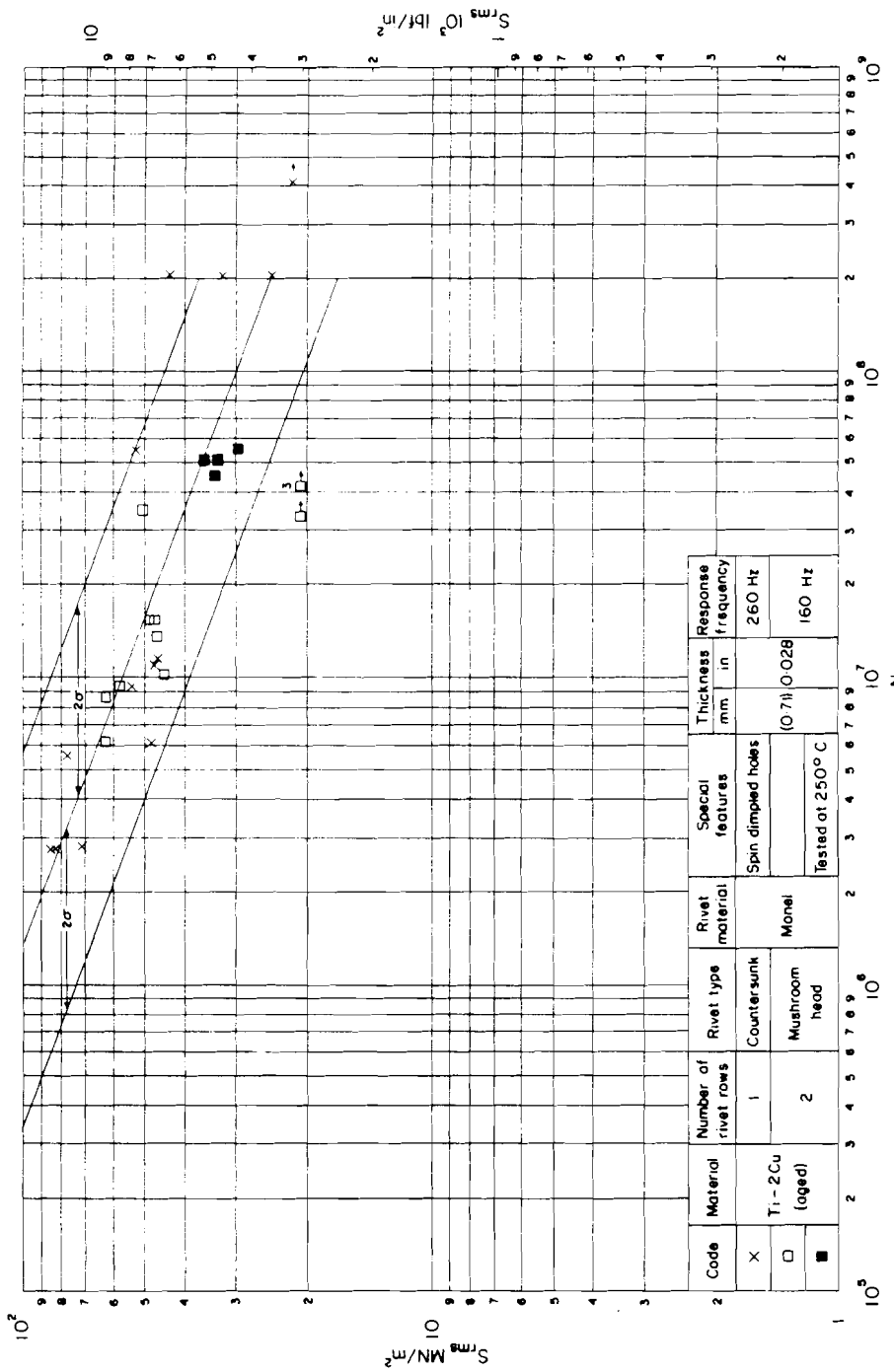

FIGURE 1.3. S-N DATA FOR RIVETED SKIN IN Ti-2Cu ALLOY

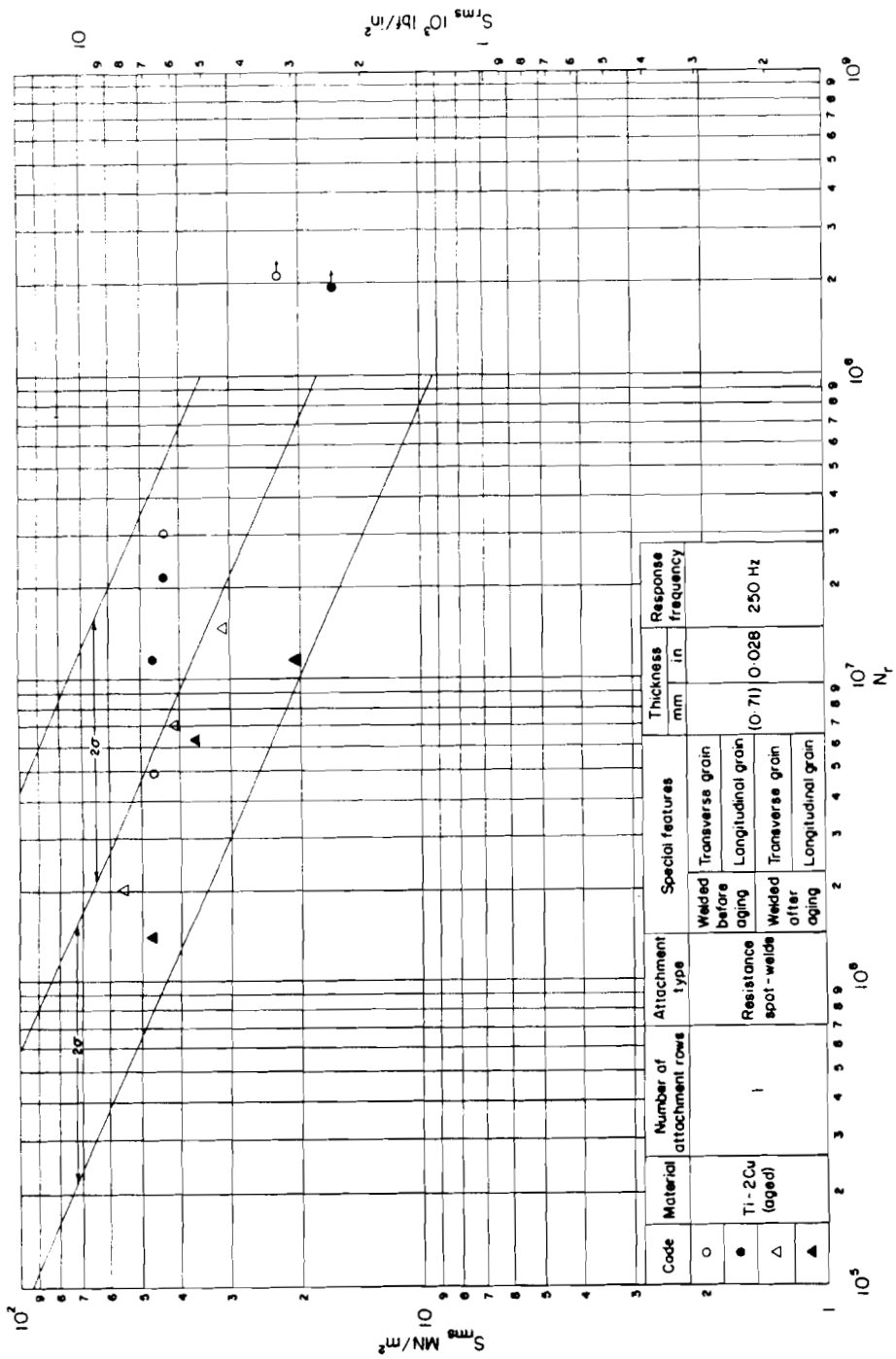

FIGURE 1.4. S-N DATA FOR SPOT-WELDED SKIN IN Ti-2Cu

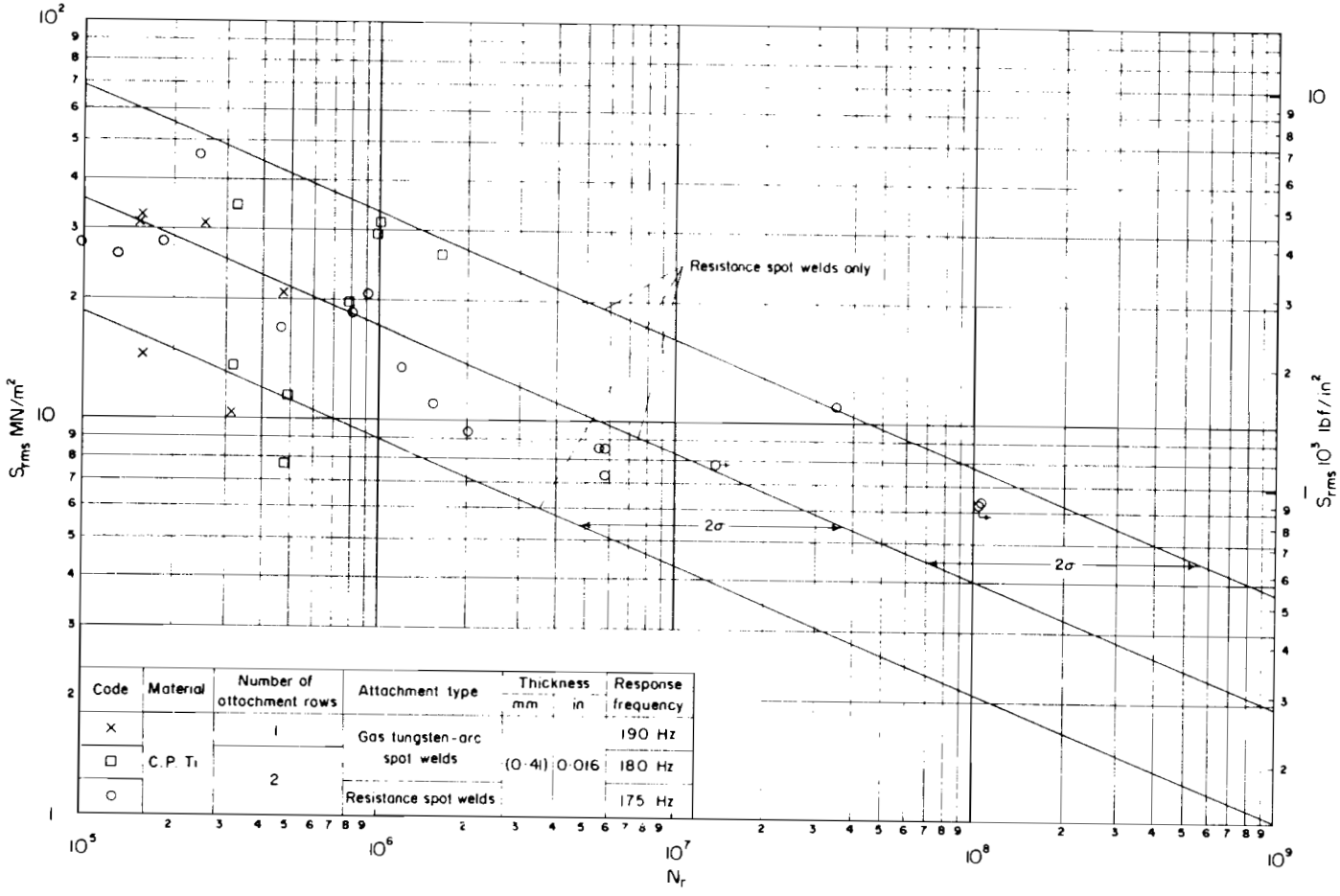

FIGURE 1.5. S-N DATA FOR SPOT WELDED SKIN IN C.P. Ti

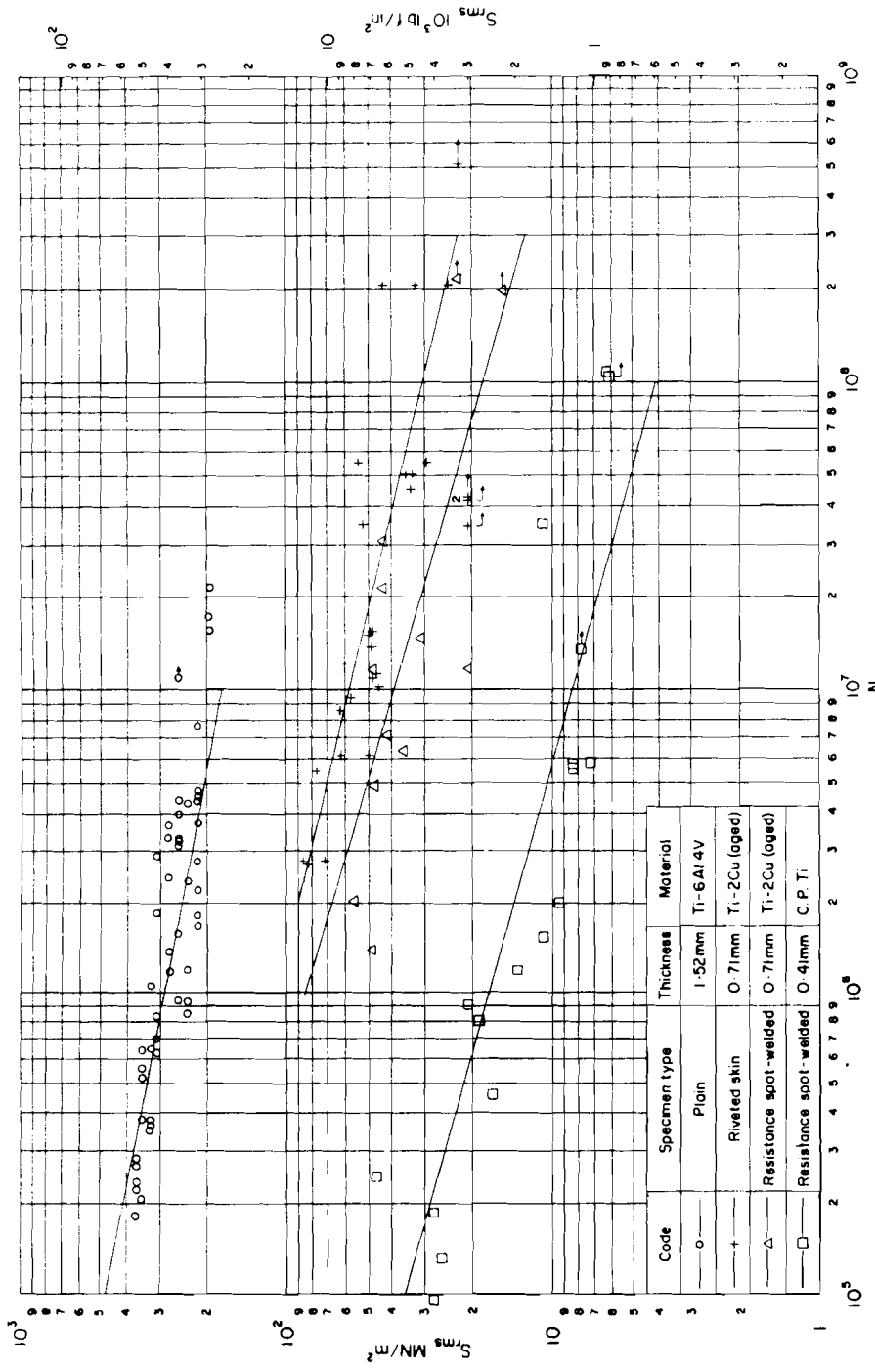

FIGURE 1.6. S-N DATA FOR ALL SPECIMENS

APPENDIX 1A

1A.1 Tests On Plain Specimens

Method of testing

Plain cantilever specimens of the type shown in Figure 1.1a, rigidly clamped at one end, were excited electromagnetically through small steel plates attached to the other ends such that they vibrated at their resonant frequency of approximately 300 Hz with a Rayleigh distribution of peak stresses truncated at ± 4 times the root mean square stress. The stress level in the specimens was monitored by a capacitive transducer, located about half-way along the specimen, which had been calibrated against strain gauges affixed at the failure location.

The random loading was interrupted at intervals to test for failure, using constant amplitude excitation, the criterion being the reduction of the resonant frequency to 98% of its original value.

1A.2 Tests On Fastened-Skin Specimens

Method of testing

Skin-stiffener specimens of the types shown in Figure 2 were clamped by the base to a moving coil vibrator fed from a white noise generator. The signal from the noise generator was filtered to a $\frac{1}{3}$ octave bandwidth centred at the fundamental resonant frequency of the specimen, so giving rise to vibration of the specimen with random amplitude at its resonant frequency. The truncation stress level was between ± 3.0 and ± 3.5 times the root mean square level. The stress level in the specimens was monitored during the tests by strain gauges located either on the expected failure line or on the centre-line of the fasteners. In the latter case, failure-line stresses were estimated using a factor determined from measurement of dynamic strain distribution across the joint.

Failure was detected by the increase in damping and a marked change in response characteristics.

1A.3 Description Of Materials

General descriptions

The designations used in this Section are descriptive of the chemical composition and condition of heat treatment of the material.

C.P.Ti

Commercially pure titanium. The material used in the tests was the high strength grade (tensile strength 620 to 770 MN/m^2 (89 600 to 112 000 lbf/in^2)) with commercial designation IMI 160. The UK specification for this material was D.T.D. 5063, but this specification was superseded in 1968 by B.S. TA6 which covers a slightly lower range of tensile strength. This material is similar to the US commercially pure titanium, Ti-75A (Specification MIL-T-9046E Type 1 Comp.B or AMS 4901).

Ti-2Cu (Aged)

This is a weldable binary titanium alloy, susceptible to age hardening, containing 2 to 3 per cent copper. The specification for the material used in the tests was BAC M.47 and the commercial designation was IMI 230 (Aged). The design tensile strength for this material is 695 MN/m^2 (100 800 lbf/in^2). The UK specification for this type of material is D.T.D. 5233. There is no US Military or AMS specification covering a similar material.

Ti-6Al 4V (Ann)

The material tested had the nominal chemical composition: 6 per cent aluminium, 4 per cent vanadium, 0.08 per cent carbon, low nitrogen and hydrogen, remainder titanium. The mechanical properties were: tensile strength, 960 MN/m^2 (139 000 lbf/in^2); yield strength, 890 MN/m^2 (129 000 lbf/in^2); elongation, 10 per cent.

The material is similar to US specification MIL-T-9046E, Type III, Comp.C (Annealed) or AMS 4911 (Annealed) or British Standard TA 10.

Section 2

DAMPING IN ACOUSTICALLY EXCITED STRUCTURES

2.1 Notes

Damping is an important parameter in defining the response of a structure to high intensity acoustic loading. Increasing this parameter provides a means of reducing the amplitudes of vibration and associated stresses in a structure. At present no reliable method for predicting damping values has been devised. In this Section the sources of damping in typical structures are described and some guidance on the range of values likely to be found on different types of structure, without special damping treatment, is provided. Also some guidance is given on methods of increasing structural damping.

Damping is the energy dissipation from a vibrating system. Two theoretical models, viscous and hysteretic, are used to represent damping. In the viscous model the energy dissipated per cycle is proportional to the product of the frequency and the square of the displacement amplitude. In the hysteretic model the energy dissipated during a harmonic vibration is independent of frequency and proportional to the square of the displacement. For structures subjected to harmonic excitation hysteretic damping may be treated as viscous damping using an equivalent damping coefficient inversely proportional to the driving frequency. In this Section the viscous damping model is used. Many terms are used to define the magnitude of damping. In this Section the measure used is the damping ratio, i.e. the ratio of the actual damping coefficient to the critical damping coefficient for the mode of vibration considered, which represents the total damping within the structure from all sources. The relationships between some common measures of damping are given in Appendix 2A.

2.2 Damping Sources

2.2.1 General

The main sources of damping of structural response, before any attempt is made to increase it by artificial means, are structural, where energy is dissipated within the structure in the form of heat, and acoustic, where energy is radiated from the structure as sound. Although it is not possible to give exact relationships between the magnitudes of structural and acoustic damping ratios, it is generally expected that, for typical aircraft structures, structural damping is dominant. Other sources are present but generally these make relatively small contributions to the overall damping.

2.2.2 Structural damping

Joints and material internal hysteresis contribute to structural damping. The internal damping of the structural material is very low in conventional light alloy materials used in aircraft construction compared with that derived from joints.

At low vibration amplitudes joint damping results from hysteresis in the joint material. As the vibration amplitude increases slip occurs in the area surrounding the rivets and damping is expected to increase non-linearly. The onset of joint slip depends on joint loading and the normal pressure between the jointed surfaces. At high vibration amplitudes there is some evidence to show that joint damping may, initially, reduce with time due to reduced friction between mating surfaces.

In a built-up structure, individual joint loadings will be different in each mode; hence the contribution to the overall damping from the joint will be different in each mode.

2.2.3 Acoustic damping

Both overall structural vibration modes and local single panel modes contribute to acoustic damping. However, it is not possible to give quantitative data for these damping values.

Damping from modes involving distortion of the whole structure is dependent on the mode of vibration and the wavelength of the radiated sound. The acoustic damping ratio for a typical mode varies with frequency as shown in Sketch (i). When the wavelength of the radiated sound is greater than the longitudinal wavelength of the vibrating mode the acoustic damping ratio is zero.

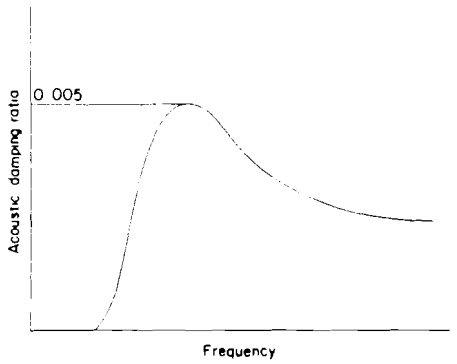

Sketch (i)

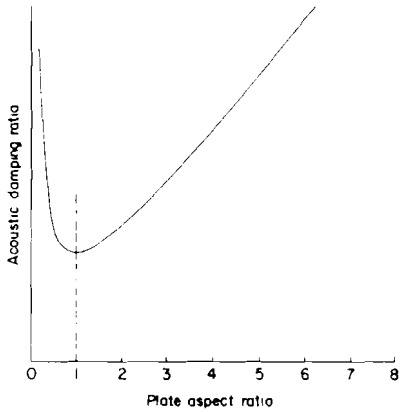

Sketch (ii)

Acoustic damping in local panel modes results from radiation from each element of the panel acting as a piston having the local velocity and amplitude of the vibrating panel. When adjacent plates, separated by a stiff edge member, vibrate in-phase the damping pressure on one plate also acts on adjacent plates increasing the overall acoustic damping ratio. If, however, adjacent plates vibrate in anti-phase their damping pressures tend to cancel each other giving a small overall acoustic damping ratio. The variation of acoustic damping ratio with plate aspect ratio for a typical rectangular plate vibrating in its fundamental mode is shown in Sketch (ii).

2.3 Damping Values for Typical Structures

2.3.1 Data presented

In Figures 2.1-2.4 the results of damping measurements made on different types of aircraft structure under discrete frequency excitation are presented. In each figure the measured damping ratio is plotted against the response frequency without differentiating between the modes of vibration. As an aid to data comparison, where sufficient measurements are available, a line is drawn through data points (using a least squares method) assuming that the damping ratio is inversely proportional to frequency.

2.3.2 Skin and stringer panels

In Figures 2.1 and 2.2 measured values of damping ratio are presented for flat and curved panels respectively. These figures demonstrate the scatter which is typical of damping measurements. The horizontal shift of the mean line on Figure 2.2, compared with Figure 2.1, may be explained by the increase in frequency due to the curvature of the panels.

The damping ratio for typical aircraft skin and stringer panels vibrating in their fundamental mode lies in the range 0.005 to 0.030.

2.3.3 Integrally-machined panels

In Figure 2.3 damping ratio is plotted against frequency for built-up structures having integrally-machined panels. The reduction in damping ratio, compared with built-up skin and stringer panels, is attributed to there being fewer joints in machined panel structures.

The damping ratio for a typical integrally-machined panel vibrating in its fundamental mode lies in the range 0.003 to 0.012.

2.3.4 Honeycomb structures

In Figure 2.4 damping ratio is plotted against frequency for flat honeycomb panels and honeycomb wedges.

The damping ratio for a typical honeycomb panel vibrating in its fundamental mode lies in the range 0.010 to 0.030.

2.4 Factors Affecting Damping

2.4.1 Structural joints

The area of contact between jointed surfaces and the normal pressure between them affects the joint load at which slip first occurs; damping is therefore dependent on the joint efficiency.

The use of a viscoelastic jointing compound can modify the stress distribution near the joint and reduce fretting but might not increase the overall damping ratio (see Figure 2.1). The separation of the metal surfaces by the jointing compound tends to prevent any reduction in damping with time resulting from oxidation of rubbing metal surfaces.

2.4.2 Frequency

Viscous damping ratios are inversely proportional to the frequency of vibration and hysteretic damping ratios are inversely proportional to the square of the frequency of vibration. As each individual damping source is most closely represented by one of the two damping models, an assemblage of all damping sources usually involves a combination of both models so that a general relationship between damping and frequency is not possible.

2.4.3 Skin Thickness

The effect of skin thickness on the damping ratio is dependent on the mode of vibration. For a stiffened panel vibrating in its stringer bending mode, damping increases with plate thickness; as plate thickness is increased damping in the stringer torsion mode passes through a maximum. Further information on the effect of skin thickness on damping is given in Derivation 2.7.4.

2.4.4 Curvature

Limited experimental data, on similar structures, suggest that curvature has little effect on the damping ratio. Curvature is likely to have the greatest effect in panel modes where stringers bend. An approximate method for estimating the effect of curvature on the damping ratio for a particular mode is given in Derivation 2.7.4.

2.4.5 Flow velocity

Air flowing past panels can reduce the damping ratio. This is important in aircraft structures where the reduction in damping may lead to panel flutter particularly in supersonic and transonic flow regions.

2.4.6 Amplitude of vibration

The variation of damping with amplitude of vibration for a typical excitation is shown in Figure 2.5. All data presented on this Figure are from one series of tests in a travelling wave tube. Damping ratios calculated using the single mode (all edges fixed) response theory are plotted against the root mean square panel stress. There is some indication that damping ratios are reduced with increase in response amplitude for these specimens, which is against the expected trend for structural damping (see Section 2.2.2). In Reference 2.7.13 data for sandwich panels show an increase in damping ratio with increase in stress amplitude.

2.5 Methods of Increasing Damping

In general, damping treatments have so far only been used on aircraft structures to alleviate a service problem not foreseen at the design stage. A better understanding of the advantages of good damping should eventually lead to its consideration as a design criterion. Consideration of damping at the design stage may allow panels with sandwiched viscoelastic material to be used which are continuous across stringer joints. However, where primary structure is concerned, there are difficulties to be overcome including loss of stiffness in joint fabrication and creep under steady load.

To increase damping in a structure efficiently, a knowledge of the frequency and shape of the modes requiring additional damping is necessary. Changing the stiffness of a structure does not improve damping unless the critical resonant frequency can be made to approach the frequency for peak acoustic damping. However increasing structural stiffness increases the natural frequencies and may thereby provide an acceptable remedy for excessive vibration if the higher frequencies are not excited during normal operating conditions.

The use of viscoelastic damping material provides the most practical method for improving damping. To be effective these materials must be applied so that they will undergo high strain. It is also necessary to select a material with suitable physical properties over the range of operating temperatures. Material properties vary greatly with temperature and are also frequency dependent. The variation of material properties with temperature for a typical viscoelastic damping compound, intended for use at normal ambient temperatures, is shown in Sketch (iii).

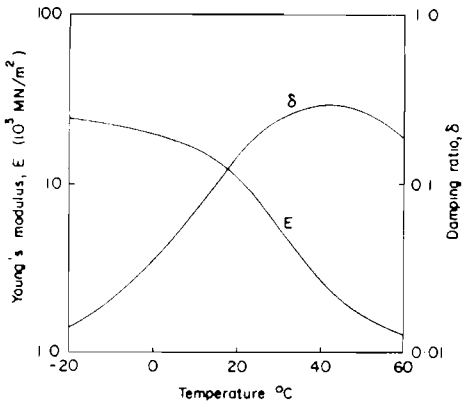

Sketch (iii)

Viscoelastic material may be applied to a structure as an unconstrained layer. For optimum damping effect the material should be placed in a region of high bending strain. The regions of highest bending strain are at the anti-node positions, and it is an advantage to have the damping material as far removed as possible from the neutral axis.

Unconstrained viscoelastic material need only be used in areas of high bending strain in the modes requiring additional damping. However, if several modes need increased damping it may be necessary to cover the whole skin surface. For stiffened panels having stiffeners of low flexural stiffness, such as integrally-machined panels, it is an advantage to use viscoelastic material on the stiffener face remote from the skin.

Constrained viscoelastic layers, formed by sandwiching damping material between skins, give increases in damping when the viscoelastic material is subjected to high shear strain. A similar constrained layer damping system is formed by attaching foil-backed damping tape to the skin surface. Expressions and calculated values for damping ratios of panels with viscoelastic damping layers are given in Derivation 2.7.7 and Reference 2.7.14.

Damping in structures may be increased by using viscoelastic inserts at joints. This method is not likely to give as high an increase in damping ratio as plate-surface layer treatments but it reduces joint fretting.

Addition of viscoelastic material leads to an increase in mass and changes in stiffness of the structure. These changes should be considered in optimising the overall effect of the damping materials.

2.6 Measurement of Damping

Damping is commonly measured from resonant response peaks, logarithmic decrement or from vector plots (see Reference 2.7.12). When natural frequencies are not well separated care is necessary to ensure that the measured damping is that for the mode required and not a combined damping ratio from a number of modes. To measure damping, instruments such as strain gauges are used which are connected by cables to recording equipment. The instrumentation and cables add to the mass and stiffness of the structure and may also cause artificial increases in damping. Because of these and other experimental difficulties, measured damping values should be considered as upper boundary values; this is particularly so when damping is measured in siren facilities when energy dissipation along the duct is likely to result in an overestimate of the true damping.

2.7 Derivation and References

Derivation

2.7.1 MEAD, D.J. The effect of a damping compound on jet-efflux excited vibrations - Part II, the reduction of vibration and stress level due to the compound. Aircr.Engng, Vol.32, No.374, pp.106-113, April 1960.

2.7.2	MEAD, D.J.	The damping, stiffness and fatigue properties of joints and configurations representative of aircraft structures. Wright Air Development Center, WADC tech.Rep.59-676, pp.235-261, March 1961.
2.7.3	MEAD, D.J.	The effect of certain damping treatments on the response of idealized aeroplane structures excited by noise. U.S. Air Force Mat.Lab. AFML-TR-65-284, August 1965.
2.7.4	MEAD, D.J.	The damping of stiffened plate structures. Acoustic fatigue in aerospace structures, pp.515-554, Syracuse University Press, 1965.
2.7.5	BALLENTINE, J.R. et al.	Refinement of sonic fatigue structural design criteria. Air Force Flight Dynamics Lab., tech.Rep. AFFDL-TR-67-156, November 1967.
2.7.6	-	Unpublished work at Dornier A.G.
2.7.7	MEAD, D.J.	The damping of jet-excited structures. Noise and acoustic fatigue in aeronautics, pp.372-379, John Wiley & Sons, 1968.
2.7.8	JONES, D.I.G. TRAPP, W.J.	Influence of additive damping on resonance of structures. J. Sound Vib., Vol.17, No.2, pp.157-185, July 1971.
2.7.9	RUDDER, F.F.	Acoustic fatigue of aircraft structural component assemblies. Air Force Flight Dynamics Lab., tech.Rep. AFFDL-TR-71-107, February 1972.
2.7.10	HAY, J.A.	Experimentally determined damping factors. AGARD-CP-113, May 1973.
2.7.11	VAN DER HEYDE, R.C.W. KOLB, A.W.	Sonic fatigue resistance of lightweight aircraft structures. AGARD-CP-113, May 1973.

References

2.7.12	KENNEDY, C.C. PANCU, C.D.P.	Use of vectors in vibration measurement and analysis. J.Aeronaut.Sci., Vol.14, No.11, pp.603-625, November 1947.
2.7.13	SWEERS, J.E.	Prediction of response and fatigue life of honeycomb sandwich panels subjected to acoustic excitation. Acoustic fatigue in aerospace structures, pp.389-401, Syracuse University Press, 1965.
2.7.14	GROOTENHUIS, P.	The control of vibration with viscoelastic materials. J. Sound Vib., Vol.11, No.4, pp.421-433, 1970.

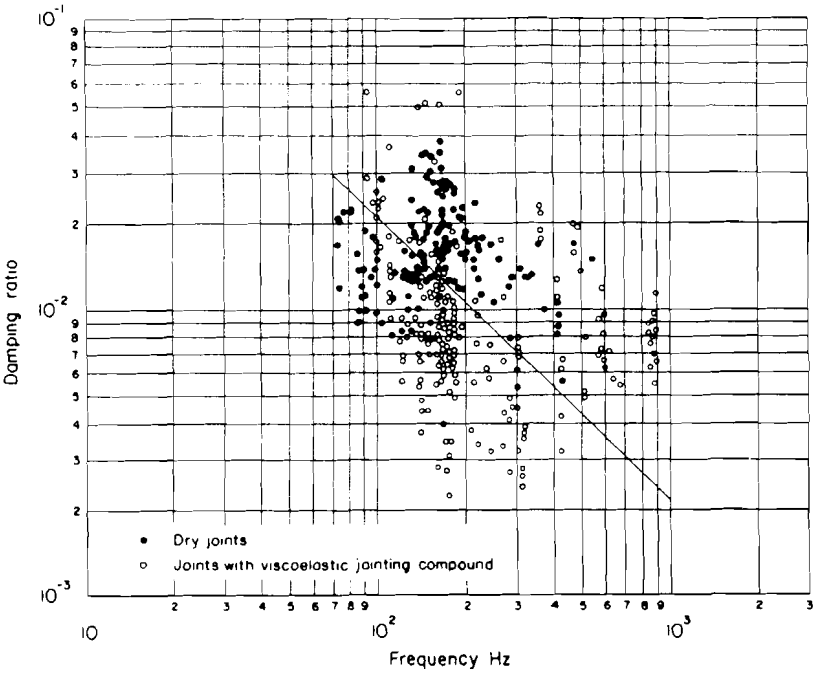

FIGURE 2.1. FLAT SKIN AND STRINGER PANELS

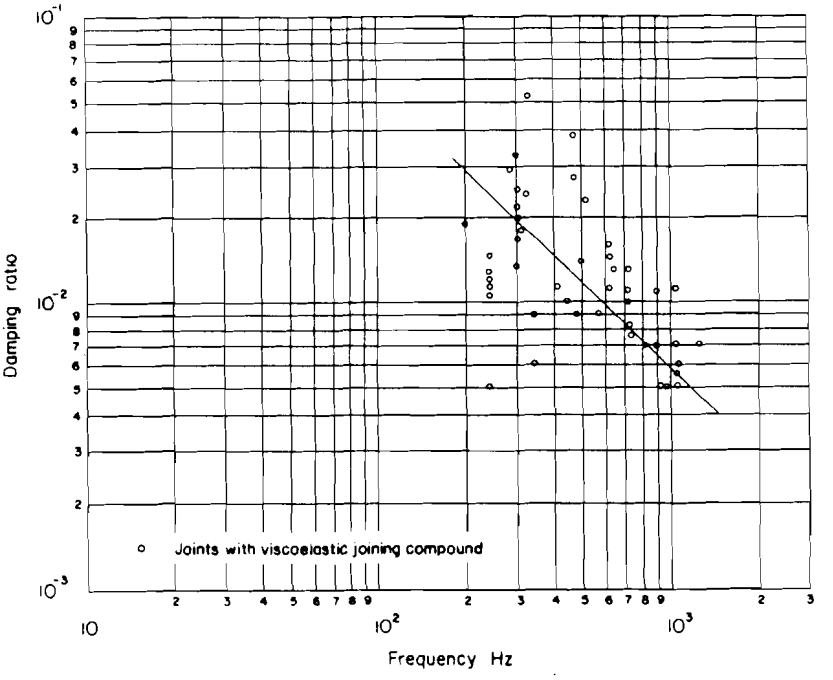

FIGURE 2.2. CURVED SKIN AND STRINGER PANELS

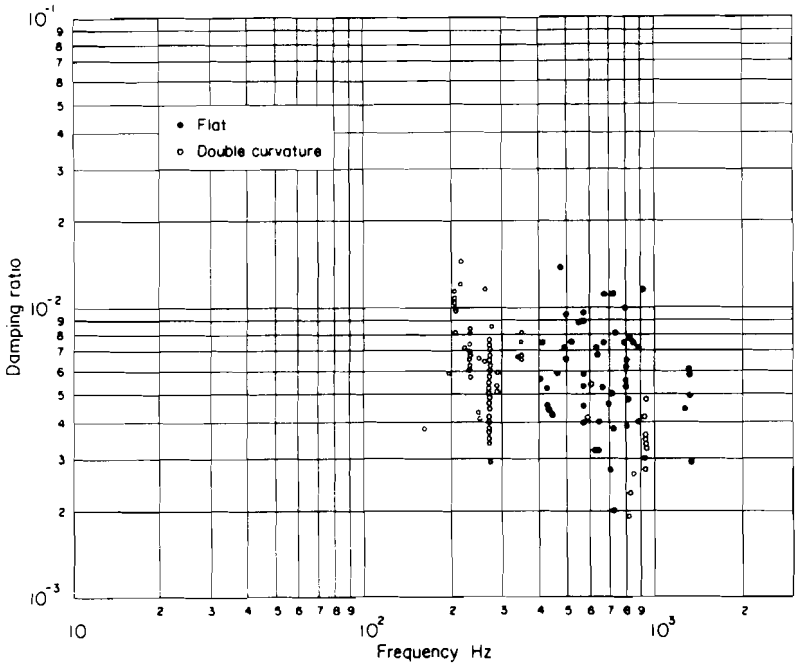

FIGURE 2.3. BUILT-UP STRUCTURES WITH INTEGRALLY MACHINED SKINS

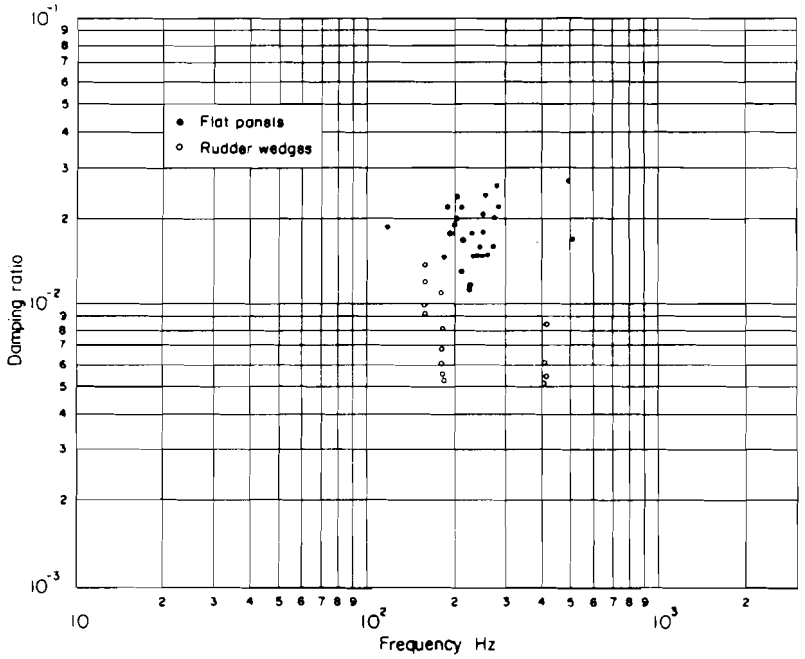

FIGURE 2.4. HONEYCOMB STRUCTURES

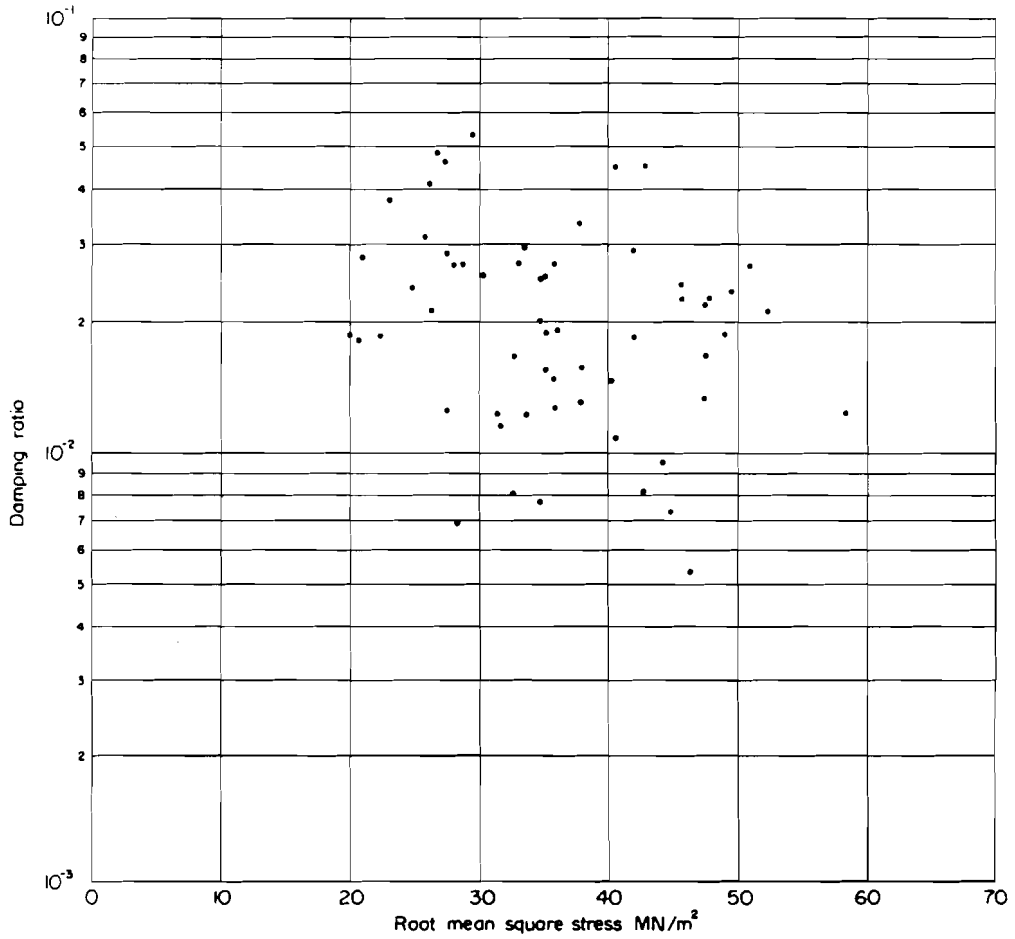

FIGURE 2.5. AMPLITUDE EFFECT ON DAMPING RATIO

APPENDIX 2A

2A.1 Notation

A_o	amplitude constant	m	in
c	damping coefficient	N s/m	lbf s/in
c_{crit}	critical damping coefficient, i.e. value of damping coefficient for which a free motion is just aperiodic	N s/m	lbf s/in
df	width of frequency response curve at which amplitude is $1/\sqrt{2}$ times maximum amplitude	Hz	c/s
F(t)	time dependent force	N	lbf
F_o	amplitude of forcing function	N	lbf
f	frequency of vibration	Hz	c/s
f_n	natural frequency of vibration	Hz	c/s
h	damping component of hysteretic stiffness	N/m	lbf/in
k	spring stiffness	N/m	lbf/in
m	mass of vibrating system	kg	lbf s^2/in
Q	magnification factor		
x, x_1, x_2	displacement	m	in
Δ	logarithmic decrement		
δ	damping ratio		
δ_H	hysteretic damping ratio		
η	loss factor		

2A.2 Damping Ratio

Considering the single degree of freedom system with a viscous damper, represented diagrammatically in Sketch 2A(i), the equation of motion of the free end of the spring relative to the unstrained position is

$$m\frac{d^2x}{dt^2} + c\frac{dx}{dt} + kx = F(t) \qquad (1)$$

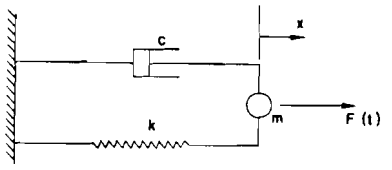

Sketch 2A(i)

The solution for free vibration (when F(t) = 0) for a lightly damped system ($\delta < 1.0$) is

$$x = A_o\, e^{-2\pi f_n \delta t}\, \cos(2\pi f_n t\sqrt{1-\delta^2}), \qquad (2)$$

where δ is the damping ratio, c/c_{crit}, and c_{crit} is given by $2\sqrt{mk}$.

2A.3 Magnification Factor

When $F(t)$ represents the harmonically varying force $F_o \cos 2 ft$, the ratio $|x| / F_o$ is equal to

$$\frac{1}{k} \frac{1}{\left[\left\{1-\left(\frac{f}{f_n}\right)^2\right\}^2 + 4\left(\frac{f}{f_n}\right)^2 \delta^2\right]^{1/2}} \qquad (3)$$

Plotting $|x| / F_o$ against f gives the frequency response curve shown in Sketch 2A(ii).

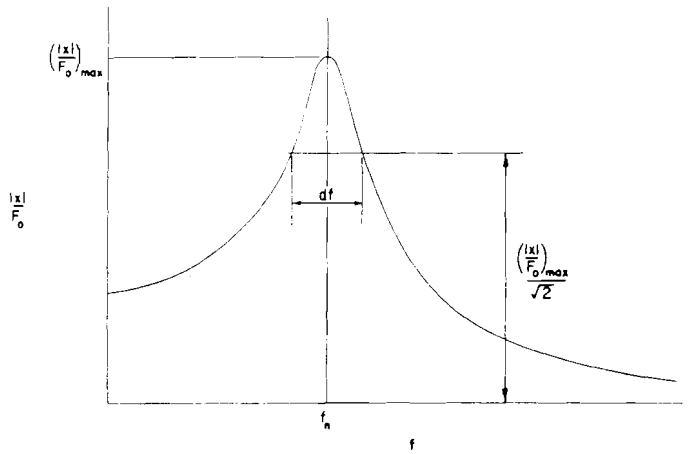

Sketch 2A(ii)

The magnification factor, Q, is the ratio of the maximum displacement (resonance value) to the static force ($f=o$) displacement. From Expression (3) it is evident that $Q = 1/2\delta$.

Provided that δ is not greater than about 0.3 it can be shown that

$$\frac{df}{f_n} = 2\delta = \frac{1}{Q} .$$

2A.4 Logarithmic Decrement

The period of the damped free oscillation of Expression (2) is $2\pi / 2\pi f_n \sqrt{1-\delta^2}$; hence the ratio of maximum amplitudes of successive cycles is given by $e^{-2\pi\delta/\sqrt{1-\delta^2}}$.

The logarithmic decrement, Δ, is given by the natural logarithm of the ratio of two successive amplitudes. The amplitudes measured at the point of tangency between the oscillation envelope and the decaying oscillation, shown in Sketch 2A(iii), closely approximate to the ratio of maximum amplitudes of successive cycles. For lightly damped systems where $\sqrt{1 - \delta^2}$ approximates to unity $\Delta = 2\pi\delta$.

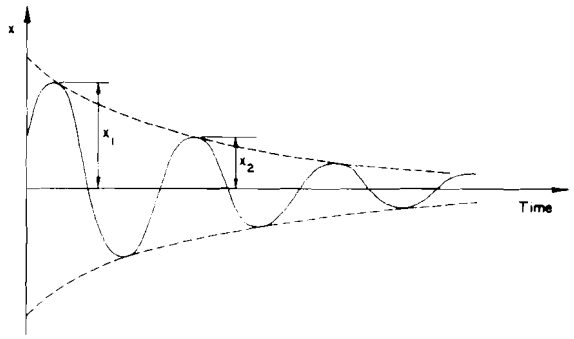

Sketch 2A(iii)

2A.5 Loss Factor

The previously defined damping values are based on a viscous damping system. For harmonically excited systems a complex stiffness type of damping can be used. The stiffness and damping forces are represented by $(k + ih)x$. This expression can be written as $(1 + i\eta)kx$ where η is the loss factor $(\eta = h/k)$.

For this type of damping

$$\frac{|x|}{F_o} = \frac{1}{k} \frac{1}{\left[\left\{1 - \left(\frac{f}{f_n}\right)^2\right\}^2 + \left(\frac{h^2}{k^2}\right)\right]^{1/2}}$$

Putting $\delta_H = h/2k$ this expression reduces to the viscous damping form.

2A.6 Damping Measure Relationship

The relationship between the viscous damping ratio and other damping measures for harmonic vibration is summarised in the table below.

Viscous damping ratio		Magnification factor		Logarithmic decrement		Loss factor
δ	$\simeq$	$\frac{1}{2Q}$	$\simeq$	$\frac{\Delta}{2\pi}$	$\simeq$	$\frac{\eta}{2}$

Section 3

REFERENCE FREQUENCY OF PANEL WITH FLEXIBLE STIFFENERS

3.1 Notation

A_s	cross-sectional area of stiffener (see Sketch (i))	m^2	in^2
a	length of longer side of plate	m	in
b	length of shorter side of plate	m	in
D	flexural rigidity of plate given by $E_p t^3/\{12(1-\sigma^2)\}$	N m	lbf in
E_p	Young's modulus of plate material	N/m^2	lbf/in^2
E_s	Young's modulus of stiffener material	N/m^2	lbf/in^2
f	reference frequency of plate	Hz	c/s
I	second moment of area of stiffener (without skin) about its neutral axis parallel to plate (see Sketch (i))	m^4	in^4
K	reference frequency parameter	m/s	in/s
t	thickness of plate	m	in
V	velocity parameter for plate material*		
σ	Poisson's ratio for plate material		
ρ	density of plate material	kg/m^3	+
ρ_s	density of stiffener material	kg/m^3	+

Both SI and British units are quoted but any coherent system of units may be used.

* The velocity parameter is defined in SI units by

$V = (E/\rho)^{1/2}/5080$ or in British units by

$V = (E/\rho)^{1/2}/200\,000$. It is approximately unity for all common structural metallic materials.

+ A density value expressed in British units as pounds per cubic inch has to be divided by 386.4 before being used to calculate parameters defined in this Section.

(A force of 1 lbf acting on a mass of 1 lb produces an acceleration of 386.4 in/s^2.)

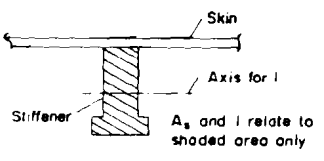

Sketch (i)

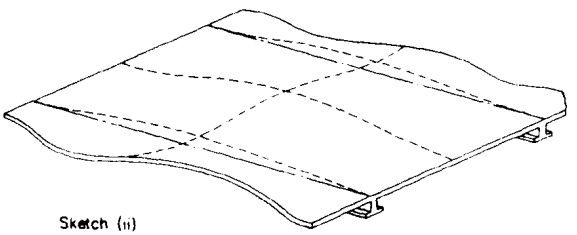

Sketch (ii)

3.2 Notes

This Section gives the reference frequency of initially unstressed, flat, uniform, rectangular plates in a panel with flexible stiffeners. The reference frequency is the fundamental natural frequency, obtained from the model used to represent the panel, where an assumed mode shape has been employed in a Rayleigh-Ritz analysis. This frequency may be used as a first approximation to the fundamental natural frequency of the plate with edges fixed against rotation. The reference frequency is intended for use in calculating the stress response of panels with flexible stiffeners under the action of acoustic loading. In the vibration mode considered the stiffeners are assumed to be free to bend in a plane normal to the plate and be fixed against rotation (see Sketch (ii)).

The reference frequency is given by

$$f = VK \frac{t}{b^2} \quad . \qquad (1)$$

In Figures 3.1-3.4 values of K are plotted against $E_s I/Db$ for a range of values of a/b. Each of these figures is drawn for a particular value of $\rho_s A_s/\rho bt$.

The plates are assumed to be separated by flexible stiffeners along their longer sides and fully fixed along their shorter sides. In the derivation stiffener bending is considered but stiffener torsion is neglected.

The use of a second moment of area of the stiffener (without skin) about its neutral axis parallel to the plate has been found to give closest correlation with limited test data. It is possible with certain configurations that the effective neutral axis could lie closer to the skin but as yet there is insufficient evidence to clarify this point.

This Section is particularly suitable for the estimation of the natural frequency of integrally-machined panels.

In deriving the curves the value of σ was assumed to be 0.3. This value gives sufficiently accurate frequencies for all common structural metallic materials.

A computer program, based on this procedure, to calculate both the reference frequency and stress response is given in Section 4 of this AGARDograph.

3.3 Comparison with Measured Data

Figure 3.5 shows a comparison of calculated reference frequency and lowest measured natural frequencies of flat stiffener panels. For some of the integrally-machined panel frequency data, where measured frequencies are taken from strain response test data, frequency bands covering the predominant response frequencies are shown.

It should be noted that in estimating frequency the plate edge-fixing approximates to the fully-fixed condition since all edges are fixed against rotation and only the ger plate edges are free in translation. With the restriction on plate edge ation the estimated frequencies are expected to be greater than the lowest measured values which correspond with modes involving stringer torsion.

3.4 Derivation

3.4.1	Ballentine, J.R. et al.	Refinement of sonic fatigue structural design criteria. Air Force Flight Dynamics Lab., Ohio, tech. Rep. AFFDL-TR-67-156, November 1967.
3.4.2	Clarkson, B.L.	Stresses in skin panels subjected to random acoustic loading. J.R.aeronaut.Soc., Vol.72, No.695, pp.1000-1010, November 1968.
3.4.3	Bayerdörfer, G. Carl, R.	Schallfestigkeitsversuche an Flugzeugstrukturen zur Erstellung von Bemessungsdiagrammen, Dornier Rep.
3.4.4	Clarkson B.L. Cicci, F.	Methods of reducing the response of integrally stiffened structures to random pressures. Trans. Am.Soc.mech.Engrs, Vol.91, Series B, No.4, pp.1203-1209, November 1969.
3.4.5	Nelson, T.F.	An investigation of the effects of surrounding structure on sonic fatigue. NASA CR-1536, May 1970.
3.4.6	Olson, M.D. Lindberg, G.M.	Jet noise excitation of an integrally stiffened panel. J.Aircr., Vol.8, No.11, pp.847-855, November 1971.
3.4.7	Rudder, F.F.	Acoustic fatigue of aircraft structural component assemblies. Air Force Flight Dynamics Lab., Ohio, tech. Rep. AFFDL-TR-71-107, February 1972.
3.4.8	Eaton, D.C.G.	Unpublished work at British Aircraft Corporation, 1973.
3.4.9	van der Heyde, R.C.W. Kolb, A.W.	Sonic fatigue resistance of lightweight aircraft structures. AGARD-CP-113, May 1973.

3.5 Example

It is required to estimate the fundamental natural frequency of a flat aluminium alloy plate in a panel array. The plate has the following dimensions and physical properties:

$A_s = 43.3\ mm^2$, $I = 950\ mm^4$,

$a = 600\ mm$, $t = 0.8\ mm$,

$b = 120\ mm$, $\sigma = 0.3$,

$E_p = E_s = 70\ 000\ MN/m^2$, $\rho = \rho_s = 2770\ kg/m^3$.

Firstly $$D = \frac{70\ 000 \times 10^6 \times (0.8 \times 10^{-3})^3}{12(1 - 0.3^2)} = 3.28\ N\ m,$$

$$\frac{a}{b} = \frac{600}{120} = 5,$$

$$\frac{\rho_s A_s}{\rho b t} = \frac{2770 \times 43.3 \times 10^{-6}}{2770 \times 120 \times 0.8 \times 10^{-6}} = 0.451,$$

and $$\frac{E_s I}{Db} = \frac{70\ 000 \times 10^6 \times 950 \times 10^{-12}}{3.28 \times 120 \times 10^{-3}} = 169.$$

From Figure 1 for $\rho_s A_s/\rho bt = 0$ $K = 2680$ m/s

from Figure 2 for $\rho_s A_s/\rho bt = 1.0$ $K = 1980$ m/s

and from Figure 3 for $\rho_s A_s/\rho bt = 2.0$ $K = 1670$ m/s

therefore by interpolation for $\rho_s A_s/\rho bt = 0.451$ $K = 2260$ m/s.

$$V = \sqrt{\frac{70\ 000 \times 10^6}{2770}} \times \frac{1}{5080} = 0.99.$$

Hence the fundamental natural frequency of the panel is

$$0.99 \times 2260 \times \frac{0.8 \times 10^{-3}}{120^2 \times 10^{-6}} = 124\ Hz.$$

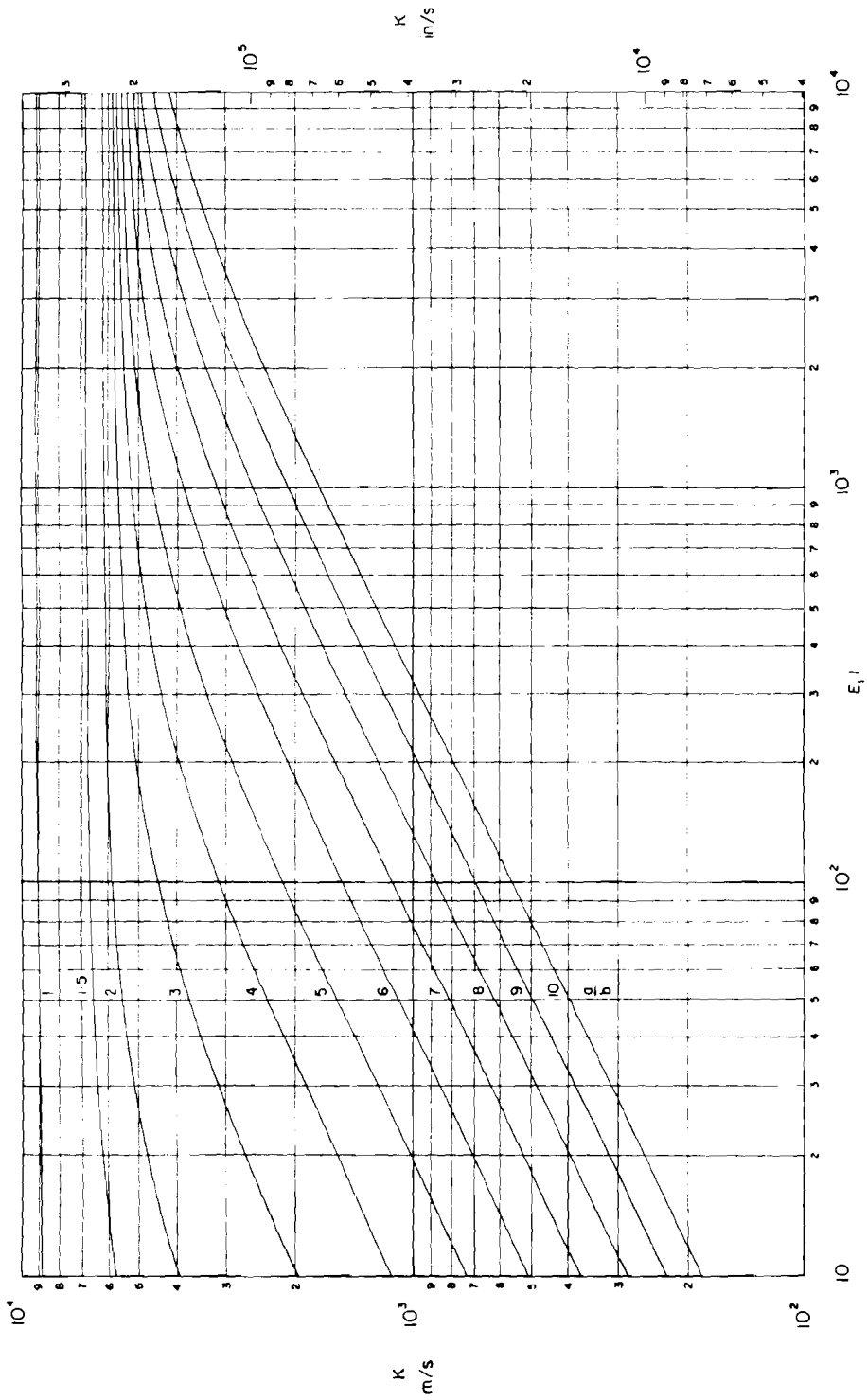

FIGURE 3.1. FREQUENCY PARAMETER FOR $\frac{\rho_1 A_1 \ell}{\rho_{DI}} = 0$

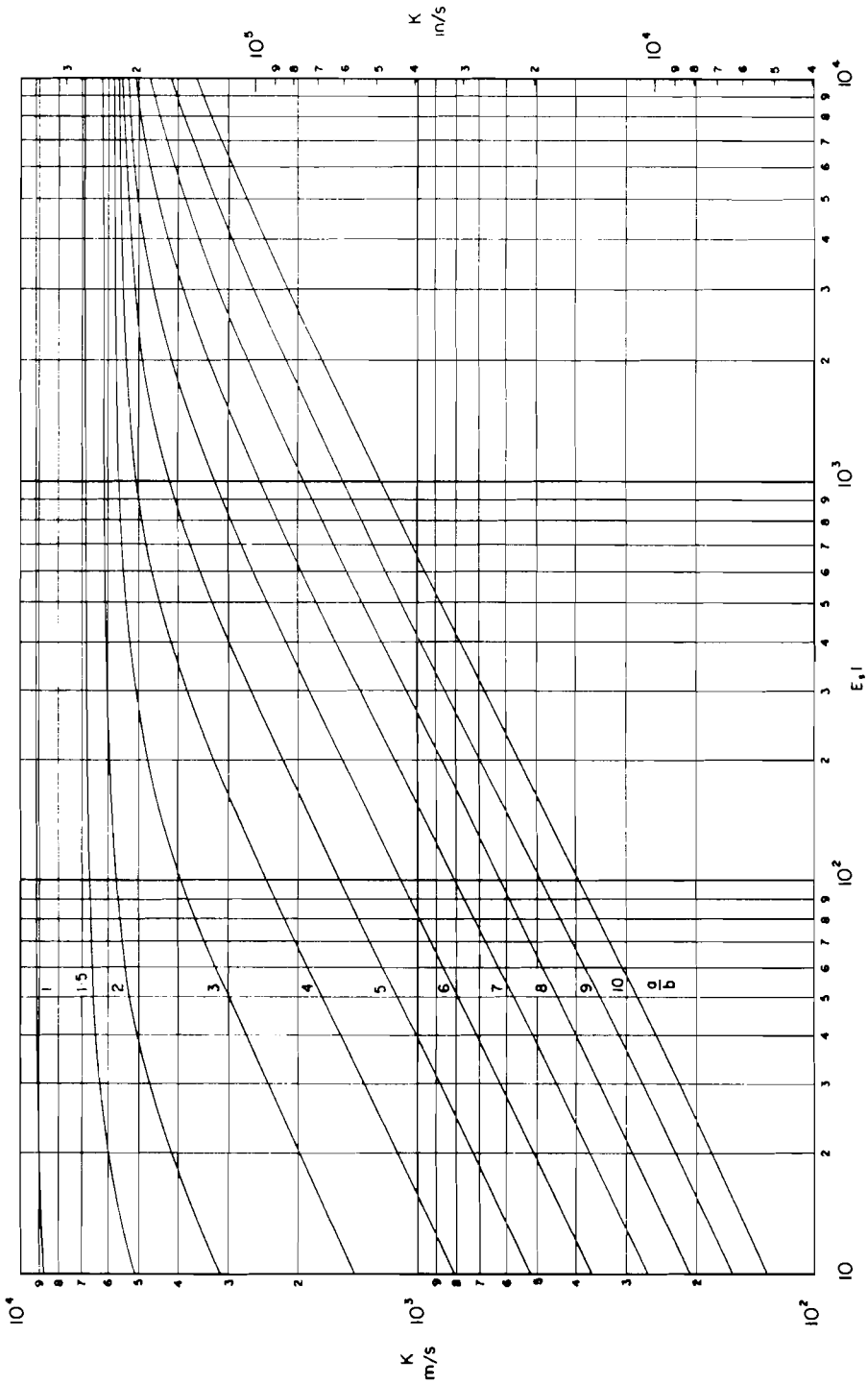

FIGURE 3.2 FREQUENCY PARAMETER FOR $\frac{\rho_s A_s}{\rho_{pb} t} = 1.0$

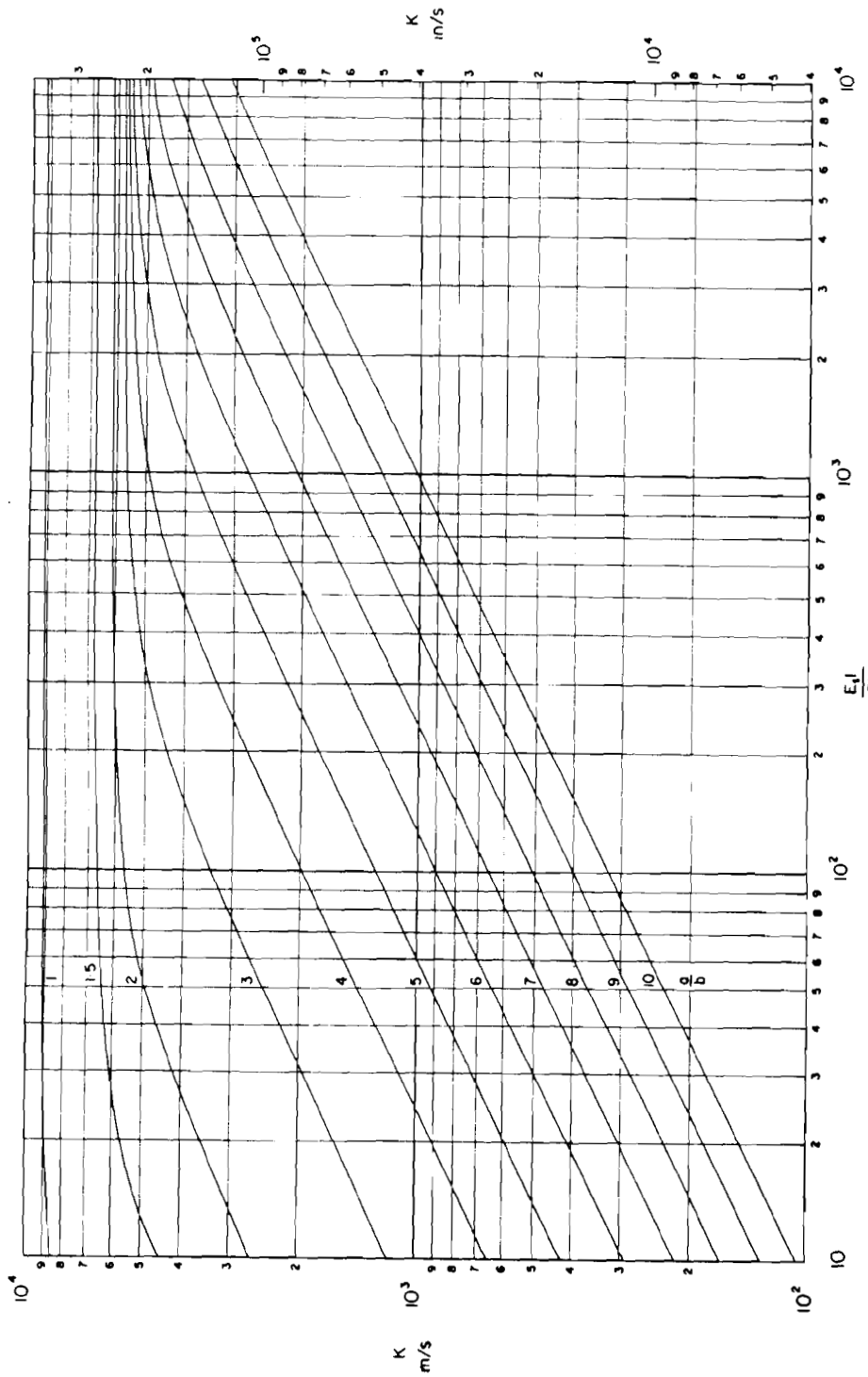

FIGURE 3.3. FREQUENCY PARAMETER FOR $\frac{\rho_s A_s}{\rho_p bt} = 2.0$

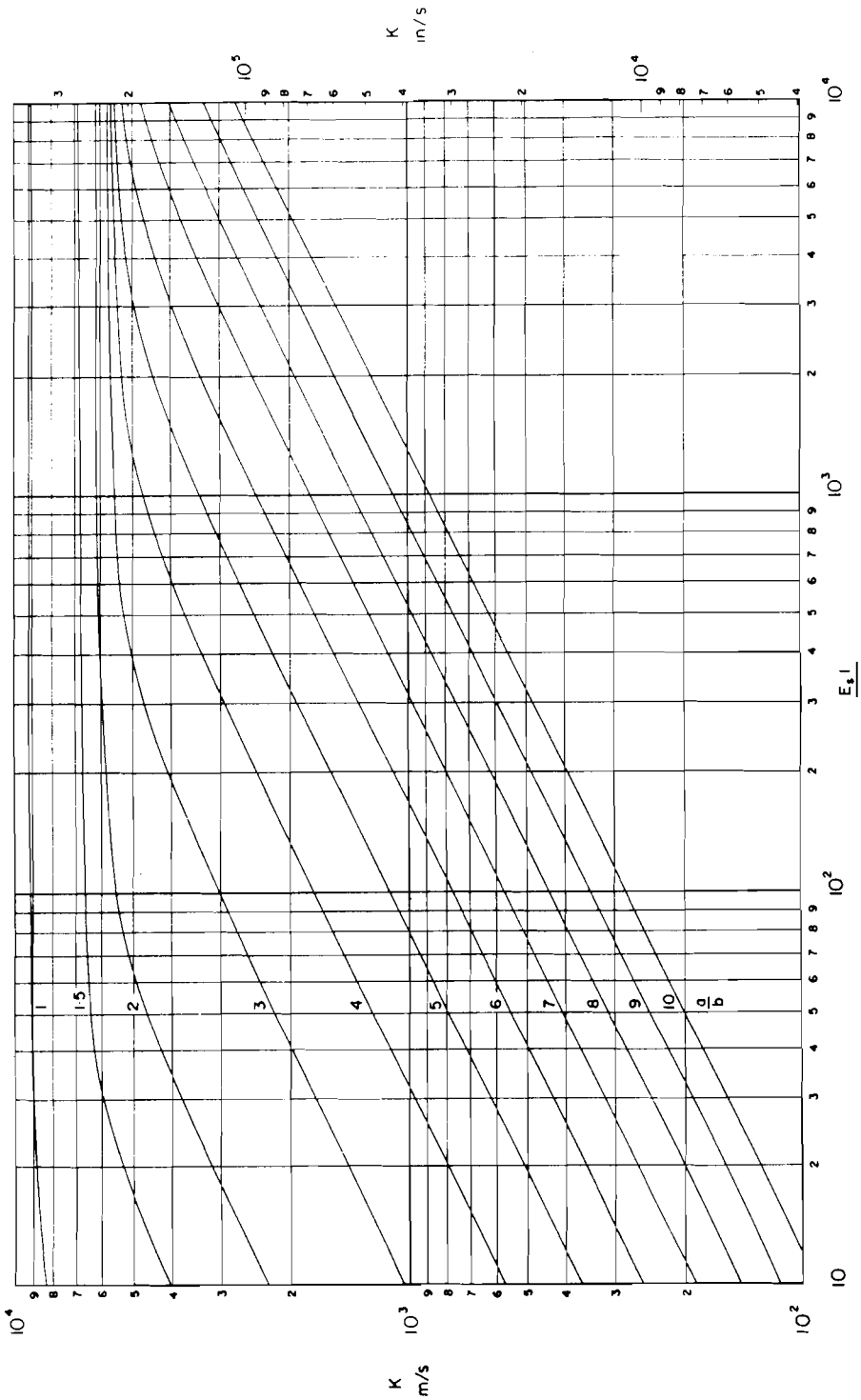

FIGURE 3.4. FREQUENCY PARAMETER FOR $\frac{\rho_s A_s}{\rho_p bt} = 3.0$

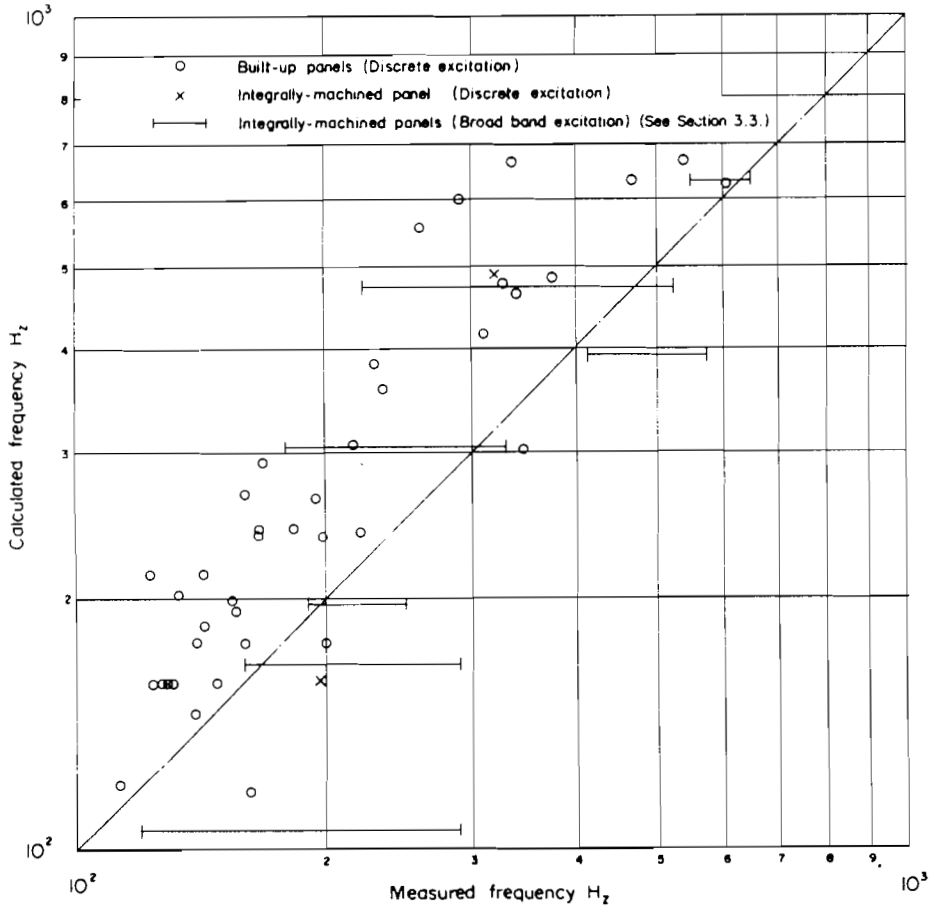

FIGURE 3.5. COMPARISON OF CALCULATED AND MEASURED FREQUENCIES

Section 4

THE ESTIMATION OF R.M.S STRESS IN SKIN PANELS WITH FLEXIBLE STIFFENERS SUBJECTED TO RANDOM ACOUSTIC LOADING

4.1 Notation

A_s	cross-sectional area of stiffener (see Sketch (i))	m^2	in^2
a	length of longer side of plate	m	in
b	length of shorter side of plate	m	in
D	plate flexural rigidity given by $E_p t^3/\{12(1-\sigma^2)\}$	N m	lbf in
d	height of stiffener	m	in
E_p	Young's modulus of plate material	N/m^2	lbf/in^2
E_s	Young's modulus of stiffener material	N/m^2	lbf/in^2
f	fundamental natural frequency of panel with edges fixed against rotation	Hz	c/s
$G_p(f)$	spectral density of acoustic pressures at frequency f	$(N/m^2)^2/Hz$	$(lbf/in^2)^2/(c/s)$
I	second moment of area of stiffener (without skin) about its neutral axis parallel to plate (see Sketch (i))		
K'	stress parameter (for plate stresses $K'=K_n$ and for stiffener stress $K'=(E_s/E_p)(d/t)K_s$)		
K_n	plate stress parameter (n=1-5 and denotes location of plate stress - see Sketch (ii))		
K_s	stiffener stress parameter		
K_δ	damping ratio correction factor		
$L_{ps}(f)$	spectrum level of acoustic pressure at frequency f	dB	dB
p	uniform static pressure on plate	N/m^2	lbf/in^2
p_{rms}	root mean square fluctuating pressure	N/m^2	lbf/in^2
S_o	ratio of stress at considered plate location to applied uniform static pressure on plate		
S_{rms}	r.m.s. stress at stiffener due to acoustic loading	N/m^2	lbf/in^2
t	thickness of plate	m	in
δ	damping ratio in vibrating mode		
δ_{ref}	reference damping ratio (=0.017)		

ρ	density of plate material	kg/m^3	+
ρ_s	density of stiffener material	kg/m^3	+
σ	Poisson's ratio for plate material		

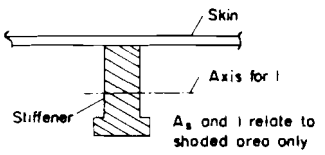

Sketch (i)

Both SI and British units are quoted but any coherent system of units may be used.

+A density value expressed in British units as pounds per cubic inch has to be divided by 386.4 before being used to calculate parameters defined in this Section. (A force of 1 lbf acting on a mass of 1 lb produces an acceleration of 386.4 in/s^2.)

4.2 Notes

This Section gives a method of estimating the r.m.s. stress in flat rectangular skin panels with flexible stiffeners under the action of random acoustic loading. The stress locations on the plate and stiffener, and directions of r.m.s. stress, for which values are provided are shown in Sketch (ii).

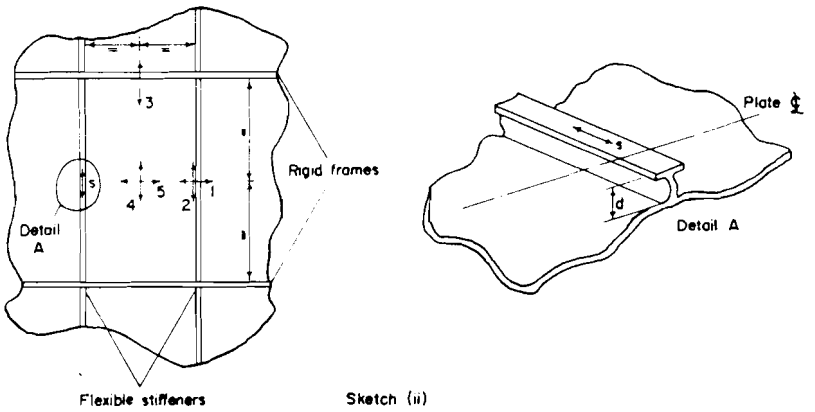

Sketch (ii)

The r.m.s. stress for a stiffened panel subjected to random acoustic loading one side is given approximately by the expression

$$S_{rms} = \left[\frac{\pi}{4\delta_{ref}} f G_p(f) \right]^{1/2} K_\delta S_o, \qquad 4.1$$

when only the fundamental natural mode is excited by the noise. For plate stresses the ratio S_o is proportional to the product of a stress parameter and $(a/t)^2$ and for the stiffener stress S_o is proportional to the product of a stress parameter, $(a/t)^2$ and (d/t). In Figures 4.1-4.20 values of K_n are plotted against $E_s I/Db$ for a range of values of a/b. Similarly in Figures 4.21-4.24 values of K_s are presented. Each of these Figures is drawn for a particular value of $\rho_s A_s/\rho bt$ as detailed in Table 4.1.

TABLE 4.1

Stress location \ $\frac{\rho_s A_s}{\rho bt}$	Figure nos. for stress parameter			
	0	1	2	3
1	4.1	4.2	4.3	4.4
2	4.5	4.6	4.7	4.8
3	4.9	4.10	4.11	4.12
4	4.13	4.14	4.15	4.16
5	4.17	4.18	4.19	4.20
S	4.21	4.22	4.23	4.24

Figures 4.25 and 4.26 give nomographs for S_{rms}. The nomographs are entered at a value of $L_{ps}(f)$, each quadrant being used in turn in the direction indicated through ranges of a/t, K' and f. Figure 4.26 is an extension of the stress range of Figure 4.25. The stress nomographs are drawn for a value of $\delta = 0.017$; S_{rms} for other values of δ is calculated using a correction factor K_δ which is plotted against δ in Figure 4.27. Guidance on values of δ for typical aircraft structures may be found in Section 2 of this AGARDograph.

The use of a second moment of area of the stiffener (without skin) about its neutral axis parallel to the plate has been found to give closest correlation with limited test data. It is possible with certain configurations that the effective neutral axis could lie closer to the skin but as yet there is insufficient evidence to clarify this point.

For panels with riveted stiffeners the edge stresses may be used as the nominal unfactored rivet line values. In using these stresses to calculate a fatigue life care must be taken to ensure that fatigue data from a similar structure are used so that geometric stress concentration factors are of the same order.

In obtaining values of K_n and K_s presented in Figures 4.1-4.24 the panels were assumed to be built-up from plates fully fixed on their shorter sides, and attached to flexible stiffeners along their longer sides. The assumed deflected shape is shown in Sketch (iii). At plate locations 1 and 2 the value of K_n, for plates having high aspect ratio and very flexible stiffeners, reduces to zero and then increases as $E_s I/Db$ increases. This is due to the change in sign of the static stress ratio as the relative stiffness of the plate to that of the stiffener increases. The number of individual plates in the panel array, between each pair of rigid supports or stiff frames, was taken to be sufficiently great for the centre panel of the array to be unaffected by the number of plates in the panel.

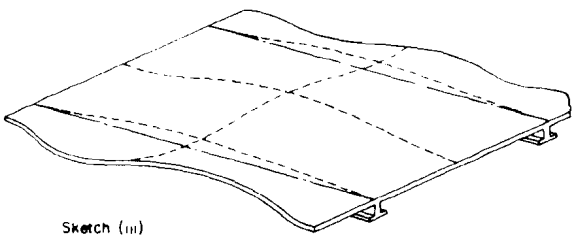

Sketch (iii)

The pressure is assumed to be uniform and in phase over the whole of each individual plate and the spectrum level of the acoustic pressure is taken to be constant over the range of frequencies close to the fundamental natural frequency of the panel.

In the derivation of the nomograph it is assumed that the plate bending stress is within the linear region where it is directly proportional to the normal pressure, that is p/E_p less than about $20(t/b)^4$ (see Reference 4.5.10). Also the value of δ is taken to be 0.3; use of this value gives a sufficiently accurate stress for all common structural metallic materials.

For conventional structures without special damping treatment f should be taken as the undamped natural frequency.

This Section is particularly applicable to integrally-machine panel structures.

In Appendix 4A a computer program, based on the procedure of this Section and Section 3, is described which calculates the fundamental natural frequency and stress response to acoustic loading of panels with flexible stiffeners. Sub-routines are given for both the frequency and stress calculations.

4.3 Calculation Procedure

4.3.1 The procedure for estimating S_{rms} in the general case is as follows.

(i) Estimate the reference frequency of the panel using Section 3 of this AGARDograph. This reference frequency may be taken as the fundamental natural frequency for the purpose of calculating stress.

(ii) Obtain the value of spectrum level of acoustic pressure $L_{ps}(f)$ at the calculated frequency. If only the band pressure level is known, it is first corrected to pressure spectrum level (unit bandwidth) using Reference 4.5.8. The reference pressure for sound pressure level is $20\ \mu N/m^2$.

(iii) Calculate the parameters a/b, E_sI/Db and $\rho_sA_s/\rho bt$ and from Figures 4.1-4.24 obtain the approprate value of K' or K_s.

(iv) For stiffener S_{rms} calculate the parameter $(E_s/E_p)(d/t)$ and factor K_s by that parameter to obtain the required value of K'.

(v) Calculate the parameter a/t and read the value of S_{rms} from Figure 4.25 or 4.26. The nomographs are entered at a value of $L_{ps}(f)$, each quadrant being used in turn in the direction indicated through ranges of a/t, K' and f.

(vi) For values of δ other than 0.017, factor the estimated value of S_{rms} by K_δ obtained from Figure 4.27.

4.3.2 Within the nomograph the spectrum sound pressure level is converted into the spectral density of acoustic pressure. The spectrum sound pressure level is converted into the root mean square fluctuating pressure in units of $(N/m^2)/Hz$ (see expression below or Reference 4.5.9) and then squared giving a value in units of $(N/m^2)^2/Hz^2$. Since unit bandwidth is used this is numerically equal to the spectral density of acoustic pressure $G_p(f)$ in units of $(N/m^2)^2/Hz$.

$$L_{ps}(f) = 20(\log_{10} p_{rms} + 4.70).$$

If $L_{ps}(f)$ is required in British units of $(lbf/in^2)^2/(c/s)$ it is given by

$$L_{ps}(f) = 20(\log_{10} p_{rms} + 8.54).$$

4.4 Comparison with Measured Data

Figure 4.28 shows a comparison of estimated and measured stresses in flat stiffened panels using the calculated frequency and assuming $\delta = 0.017$. Figure 4.29 shows a comparison of estimated and measured stresses using average measured values for f and δ.

4.5 Derivation and References

Derivation

4.5.1 Ballentine, J.R. et al. — Refinement of sonic fatigue structural design criteria. Air Force Flight Dynamics Lab., Ohio, tech, Rep. AFFDL-TR-67-156, November 1967.

4.5.2 Clarkson, B.L. — Stresses in skin panels subjected to random acoustic loading. J.R. aeronaut. Soc., Vol.72, No.695, pp.1000-1010, November 1968.

4.5.3 Bayerdörfer, G. Carl, R. — Schallfestigkeitsversuche an Flugzeugstrukturen zur Erstellung von Bemessungsdiagrammen, Dornier Rep.

4.5.4 Nelson, T.F. — An investigation of the effects of surrounding structure on sonic fatigue. NASA CR-1536, May 1970.

4.5.5 Rudder, F.F. — Acoustic fatigue of aircraft structural component assemblies. Air Force Flight Dynamics Lab., Ohio, tech. Rep. AFFDL-TR-71-107, February 1972.

4.5.6 van der Heyde, R.C.W. Kolb, A.W. — Sonic fatigue resistance of lightweight aircraft structures. AGARD-CP-113. May 1973.

4.5.7 Eaton, D.C.G. — Unpublished work at British Aircraft Corporation, 1973.

References

4.5.8 - Bandwidth correction. Engineering Sciences Data Item No. 66016, February 1966.

4.5.9 - The relation between sound pressure level and r.m.s. fluctuating pressure. Engineering Sciences Data Item No. 66018, February 1966.

4.5.10 - Elastic direct stresses and deflections for flat rectangular plates under uniformly distributed normal pressure. Engineering Sciences Data Item No. 71013, May 1971.

4.6 Example

It is required to estimate the plate surface stresses at the centre and edges on the plate centre line, and the stiffener free-edge stress at the centre of the longer plate side. The plate is an element of an internally-machined panel subjected to jet noise on one side.

The variation of sound pressure level over a range of frequencies is given in the table, sound pressure levels being 1/3 octave band levels.

Sound pressure level (dB)	151	155	156	155	153
Frequency (Hz)	50	100	200	300	500

The panel is made up from uniform plates having the following dimensions and properties:

$A_s = 43.3\ mm^2$, $I = 950\ mm^4$,

$a = 600\ mm$, $t = 0.8\ mm$,

$b = 120\ mm$, $\sigma = 0.3$,

$d = 16.2\ mm$, $\delta = 0.015$,

$E_p = E_s = 70\ 000\ MN/m^2$, $\rho = \rho_s = 2770\ kg/m^3$.

From Section 3 the fundamental natural frequency of the panel is 124 Hz.

By interpolation from the table the 1/3 octave band pressure level at 124 Hz is 155.9 dB.

From Reference 4.5.8,

$$L_{ps}(f) = 155.9 - 14.8 = 141.1\ dB.$$

Now $$D = \frac{70\ 000 \times 10^6 \times (0.8 \times 10^{-3})^3}{12\ (1-0.3^2)} = 3.28\ N\ m,$$

$$\frac{a}{b} = \frac{600}{120} = 5,$$

$$\frac{E_s I}{Db} = \frac{70\ 000 \times 10^6 \times 950 \times 10^{-12}}{3.28 \times 120 \times 10^{-3}} = 169$$

and $$\frac{\rho_s A_s}{\rho bt} = \frac{2770 \times 43.3 \times 10^{-6}}{2770 \times 120 \times 0.8 \times 10^{-6}} = 0.451.$$

Also $$\frac{a}{t} = \frac{600}{0.8} = 750 \quad \text{and} \quad \frac{d}{t} = \frac{16.2}{0.8} = 20.2.$$

From Figure 4.27, for $\delta = 0.015$, $K_\delta = 1.06$.

Plate r.m.s. stresses

From Figures 4.1-4.20 the values of K' are read for $\rho_s A_s/\rho bt = 0$ and 1 and by interpolation the values of K' for $\rho_s A_s/\rho bt = 0.451$ are found. From Figure 4.26, entering the nomograph at 141.1 dB the values of plate r.m.s. stresses are obtained as shown in the table.

	Stress parameter K'			S_{rms} MN/m^2	
Panel location	$\frac{\rho_s A_s}{\rho bt} = 0$	$\frac{\rho_s A_s}{\rho bt} = 1$	$\frac{\rho_s A_s}{\rho bt} = 0.451$	$\delta = 0.017$	$\delta = 0.015$
1	.0264	.0135	.0206	121	128
2	.0053	.0009	.0033	19.4	20.5
3	.0040	.0037	.0039	22.9	24.3
4	.0122	.0080	.0103	60.5	64.1
5	.0285	.0156	.0227	133	141

Stiffener r.m.s. stress

From Figures 4.21-4.24 the value of K_s is found as for the plate stresses. Factoring by $(E_s/E_p)(d/t)$ gives the required value of K'.

The value of r.m.s. stress is found from Figure 4.26.

Stress parameter K_s			$K' = K_s \frac{E_s}{E_p} \frac{d}{t}$	S_{rms} MN/m^2	
$\frac{\rho_s A_s}{\rho bt} = 0$	$\frac{\rho_s A_s}{\rho bt} = 1$	$\frac{\rho_s A_s}{\rho bt} = 0.451$		$\delta = 0.017$	$\delta = 0.015$
.0027	.0028	.0027	.0562	330	350

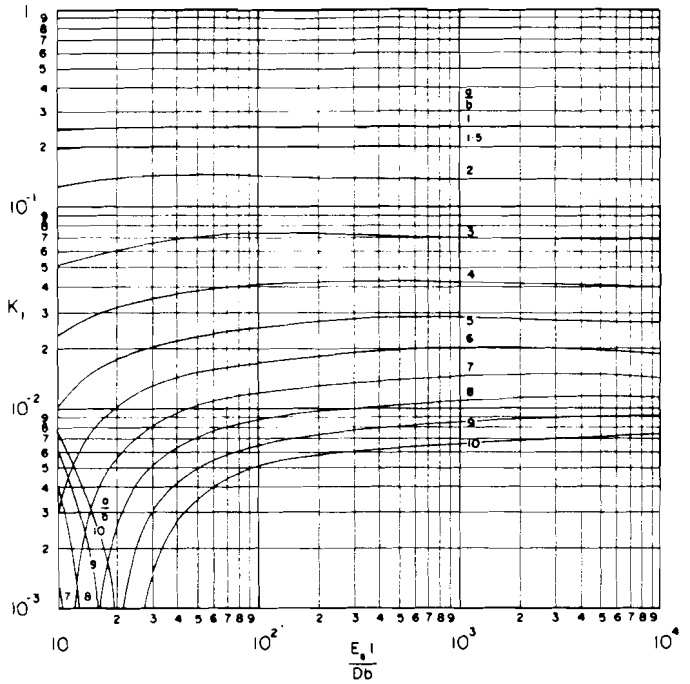

FIGURE 4.1. STRESS PARAMETER AT LOCATION 1 FOR $\rho_s A_s / \rho_p bt = 0$

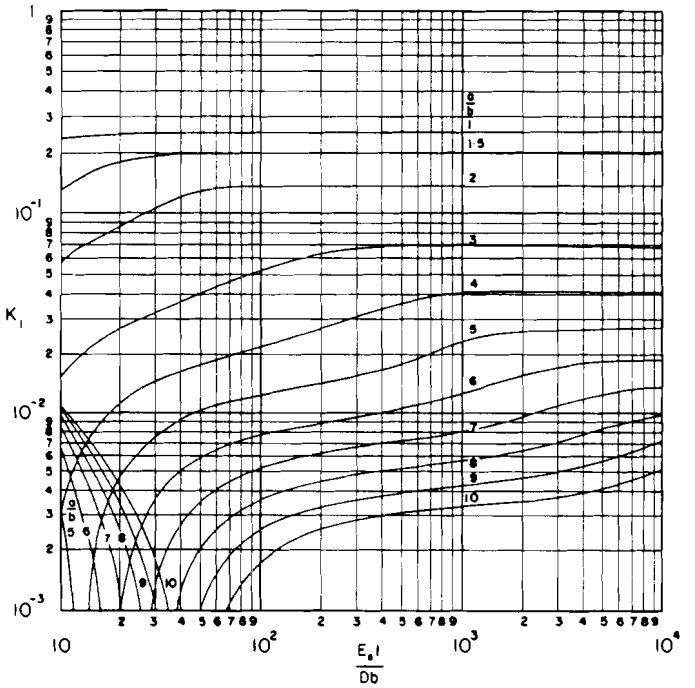

FIGURE 4.2. STRESS PARAMETER AT LOCATION 1 FOR $\rho_s A_s / \rho_p bt = 1$

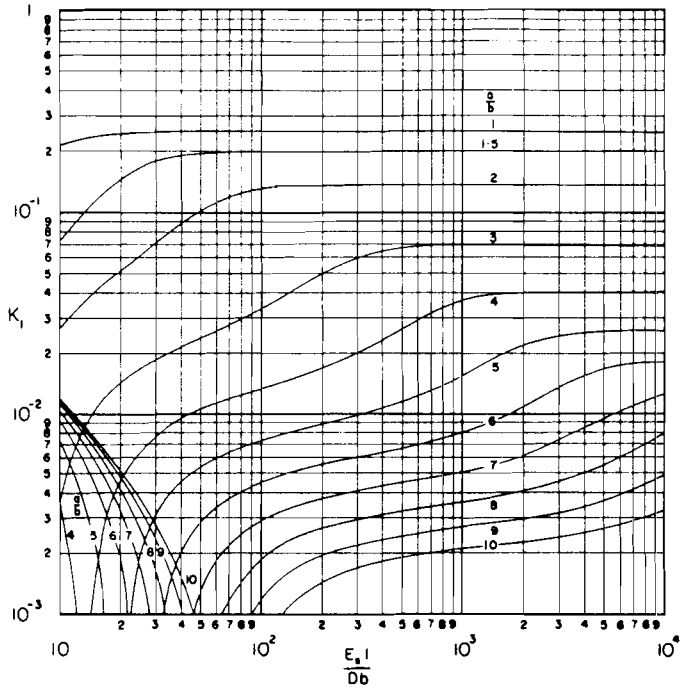

FIGURE 4.3. STRESS PARAMETER AT LOCATION 1 FOR $\rho_s A_s/\rho_p bt = 2$

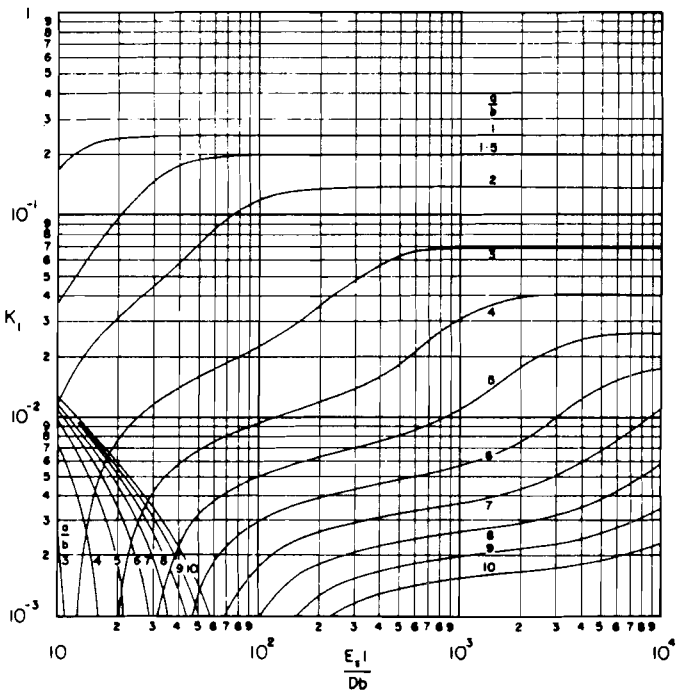

FIGURE 4.4. STRESS PARAMETER AT LOCATION 1 FOR $\rho_s A_s/\rho_p bt = 3$

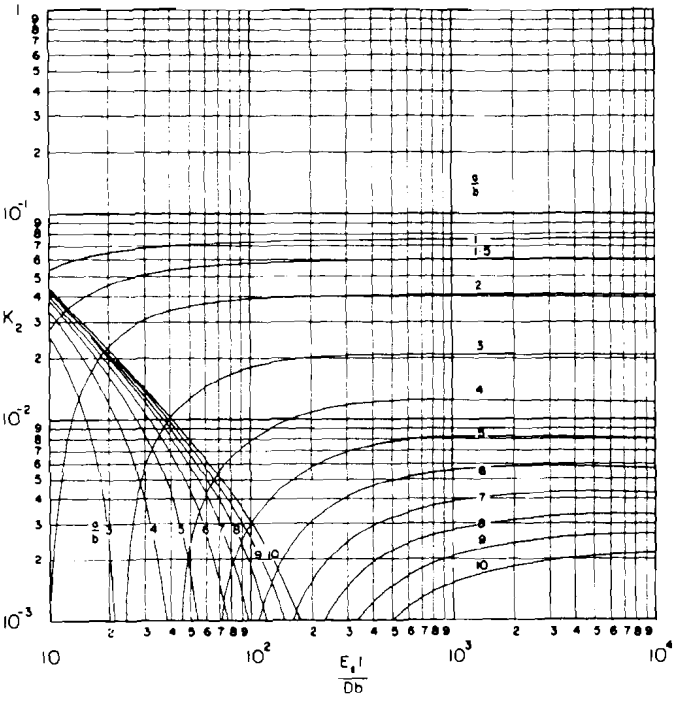

FIGURE 4.5. STRESS PARAMETER AT LOCATION 2 FOR $\rho_s A_s/\rho_p bt = 0$

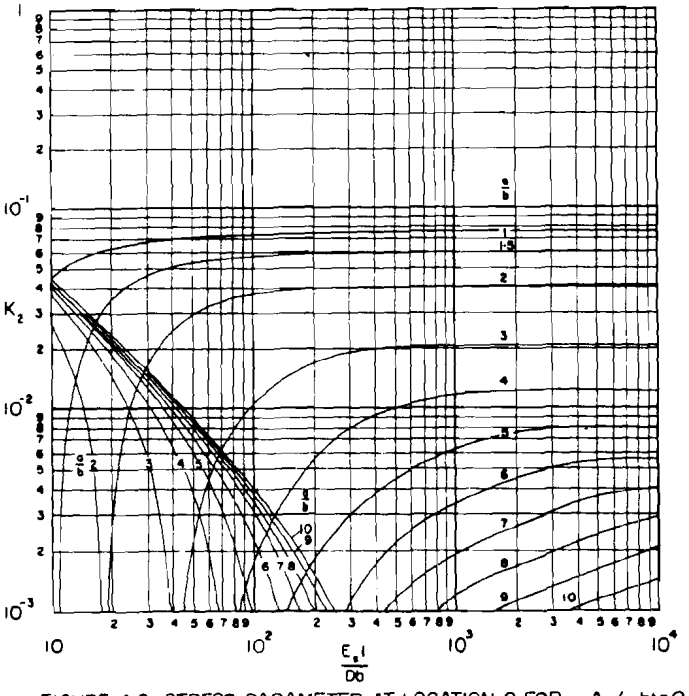

FIGURE 4.6. STRESS PARAMETER AT LOCATION 2 FOR $\rho_s A_s/\rho_p bt = 0$

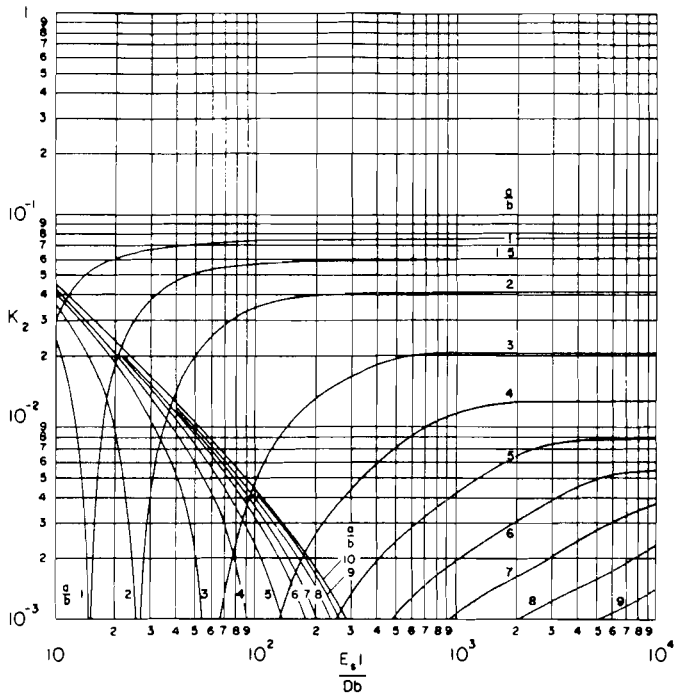

FIGURE 47 STRESS PARAMETER AT LOCATION 2 FOR $\rho_s A_s / \rho_p bt = 2$

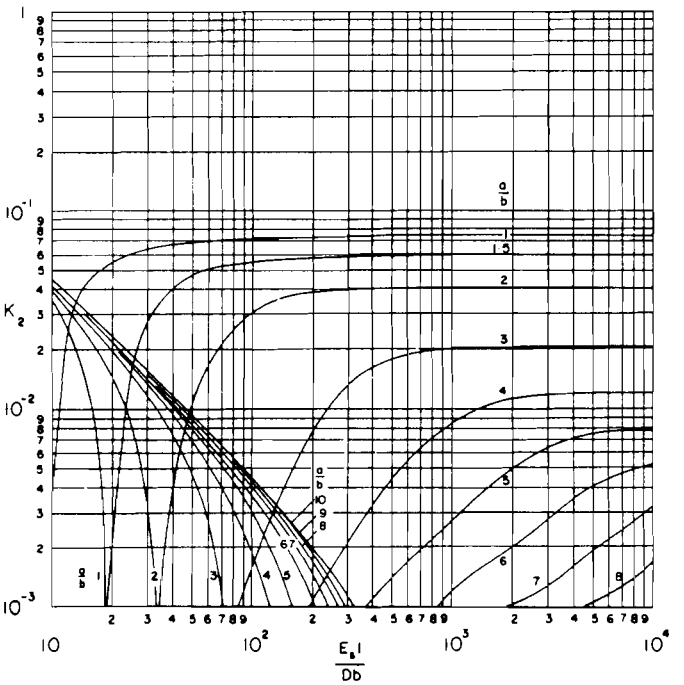

FIGURE 48 STRESS PARAMETER AT LOCATION 2 FOR $\rho_s A_s / \rho_p bt = 3$

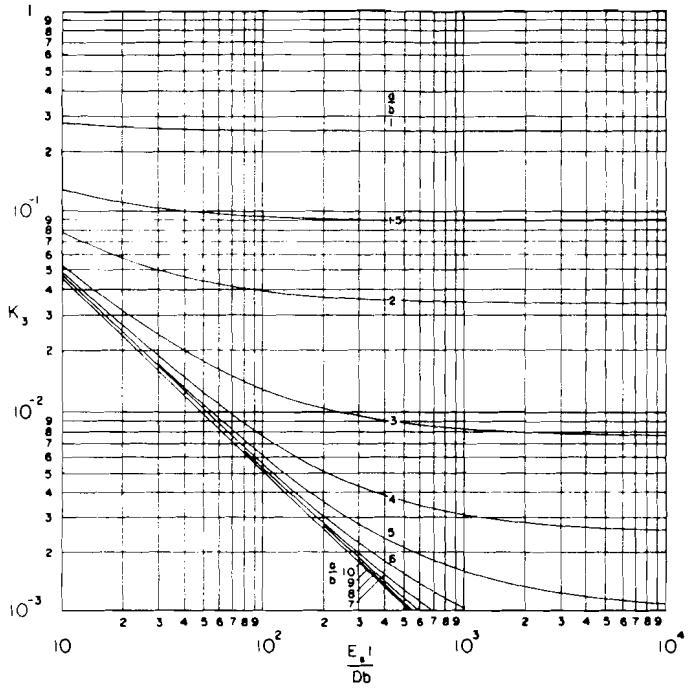

FIGURE 4.9. STRESS PARAMETER AT LOCATION 3 FOR $\rho_s A_s / \rho_p bt = 0$

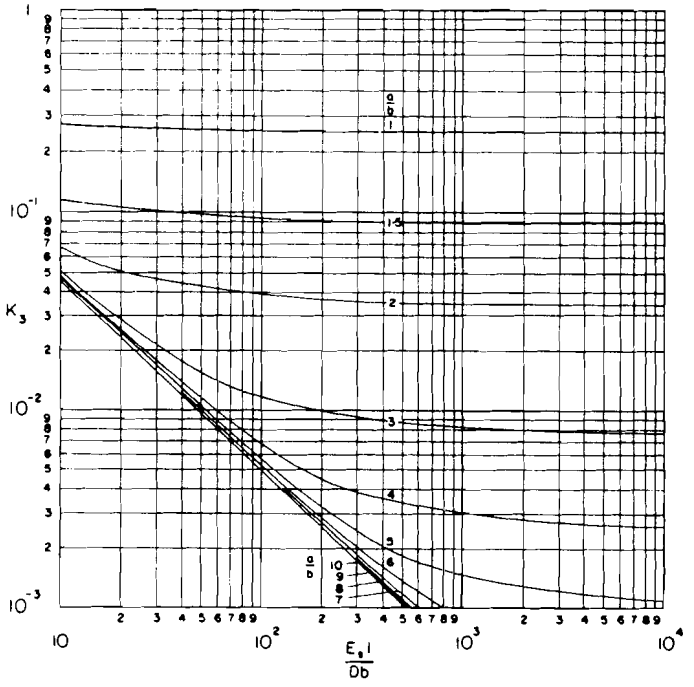

FIGURE 4.10. STRESS PARAMETER AT LOCATION 3 FOR $\rho_s A_s / \rho_p bt = 1$

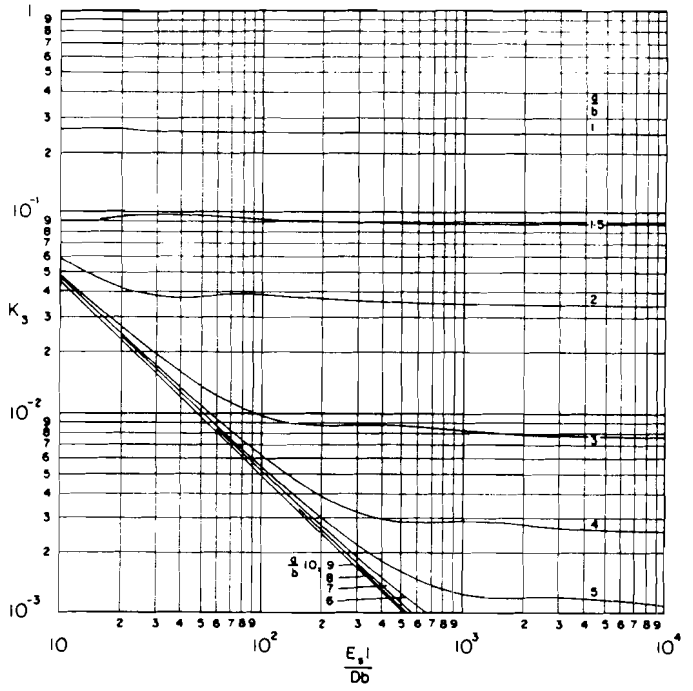

FIGURE 4.11. STRESS PARAMETER AT LOCATION 3 FOR $\rho_s A_s / \rho_p bt = 2$

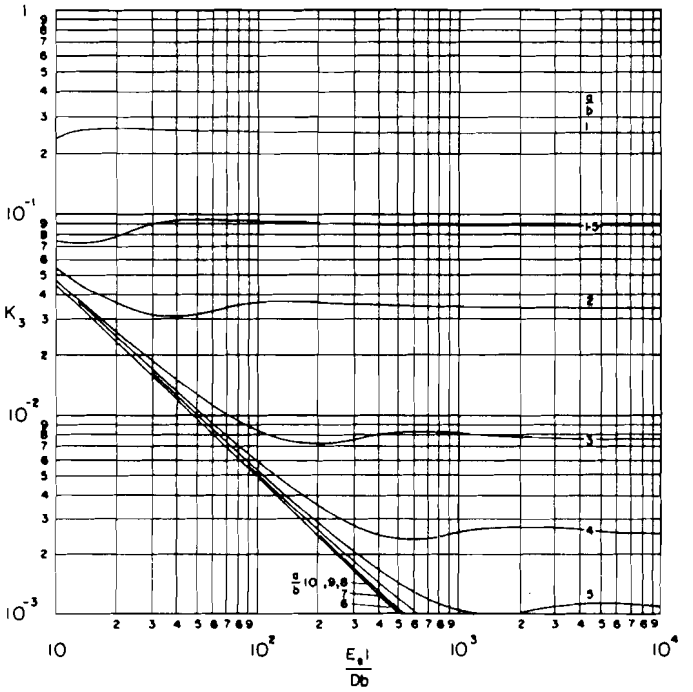

FIGURE 4.12. STRESS PARAMETER AT LOCATION 3 FOR $\rho_s A_s / \rho_p bt = 3$

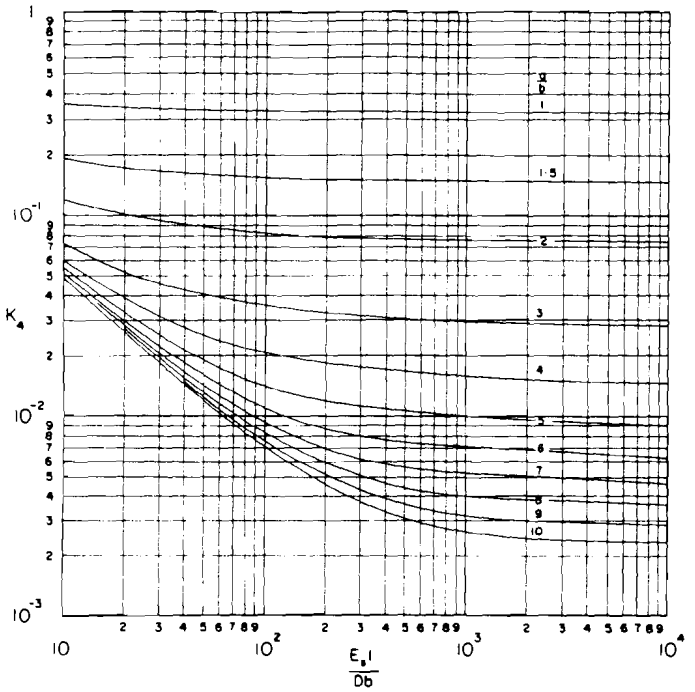

FIGURE 4.13. STRESS PARAMETER AT LOCATION 4 FOR $\rho_s A_s / \rho_p bt = 0$

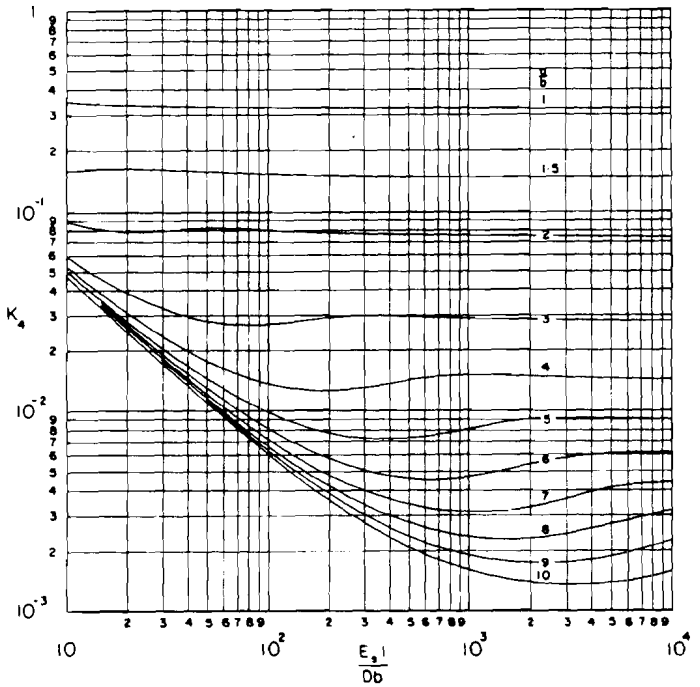

FIGURE 4.14. STRESS PARAMETER AT LOCATION 4 FOR $\rho_s A_s / \rho_p bt = 1$

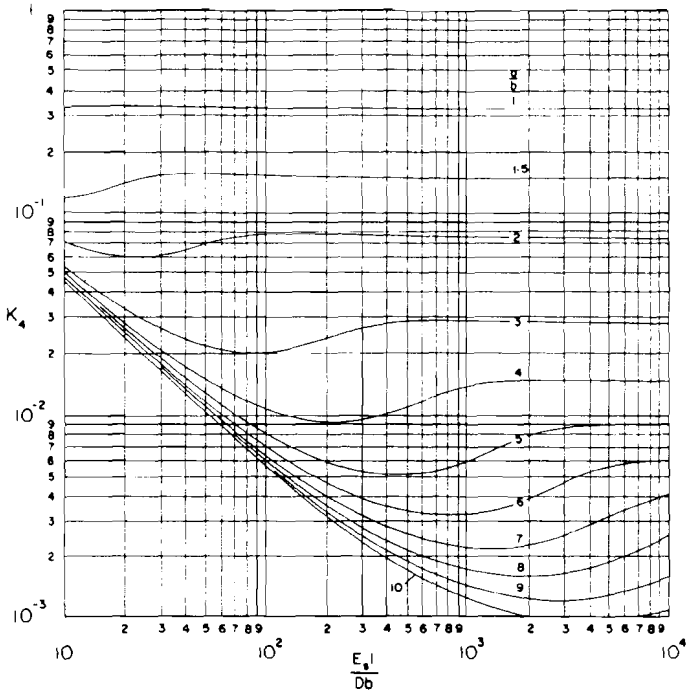

FIGURE 4.15. STRESS PARAMETER AT LOCATION 4 FOR $\rho_s A_s / \rho_p bt = 2$

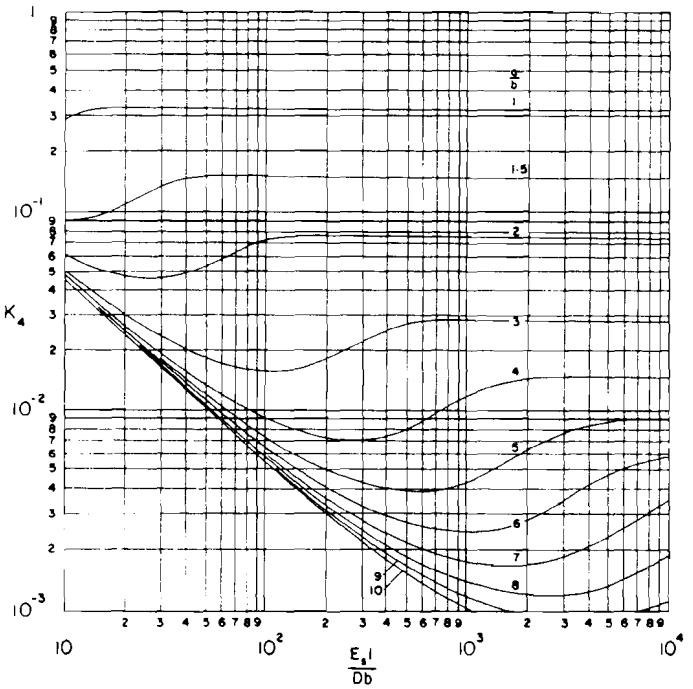

FIGURE 4.16. STRESS PARAMETER AT LOCATION 4 FOR $\rho_s A_s / \rho_p bt = 3$

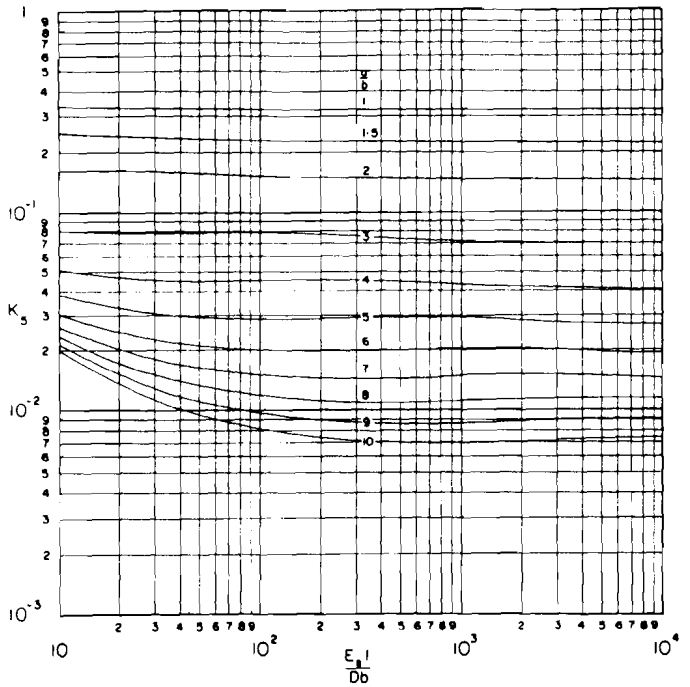

FIGURE 4.17. STRESS PARAMETER AT LOCATION S FOR $\rho_s A_s / \rho_p bt = 0$

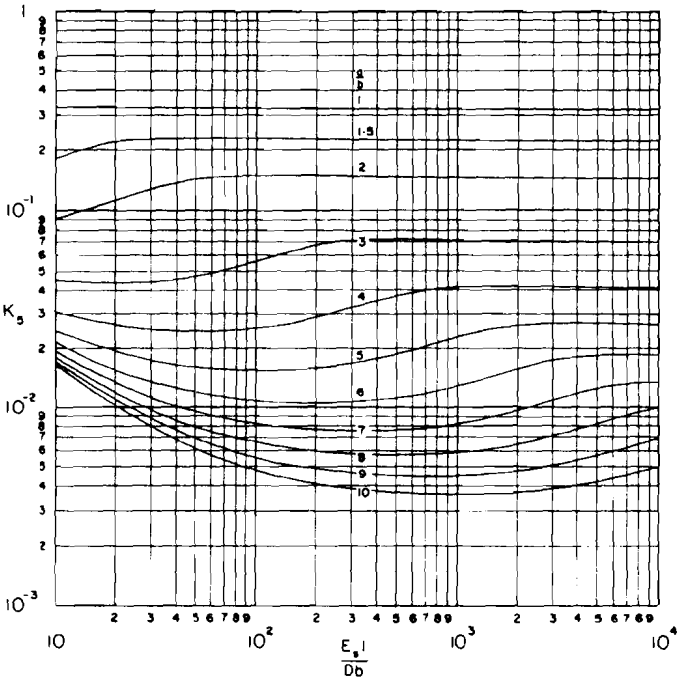

FIGURE 4.18. STRESS PARAMETER AT LOCATION S FOR $\rho_s A_s / \rho_p bt = 1$

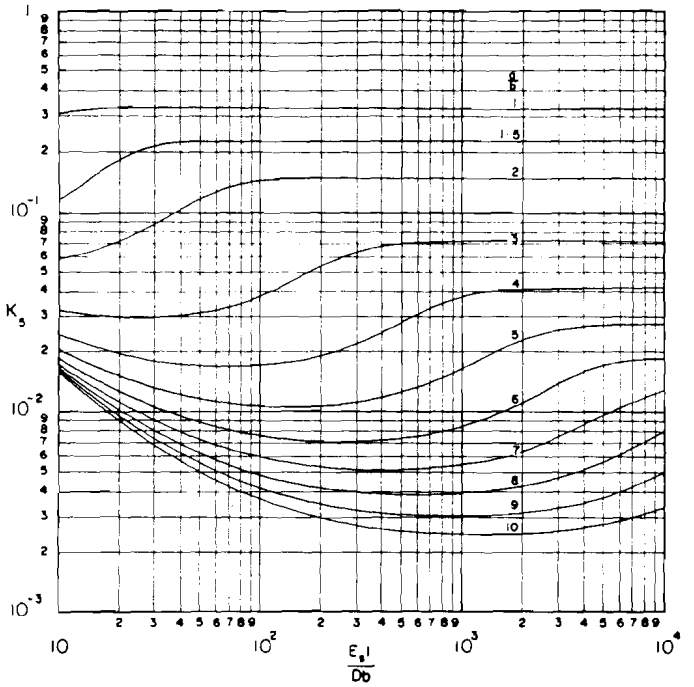

FIGURE 4.19. STRESS PARAMETER AT LOCATION 5 FOR $\rho_s A_s / \rho_p bt = 2$

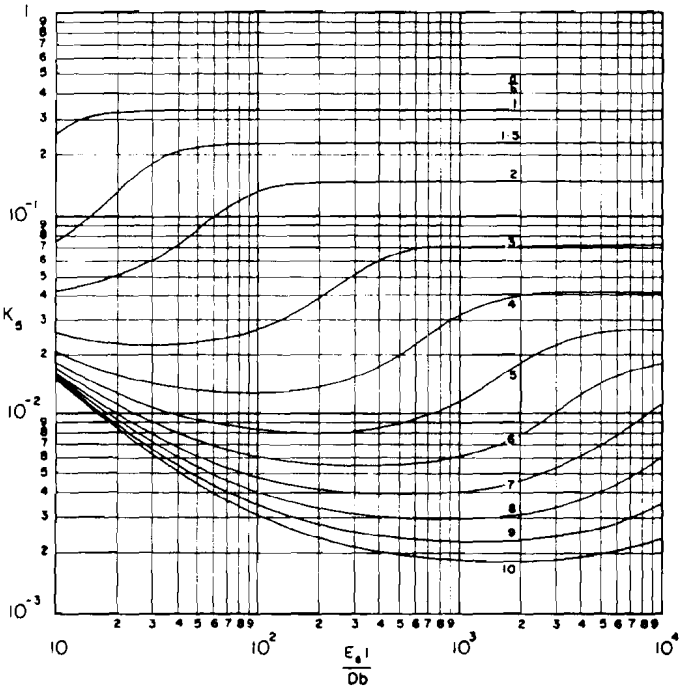

FIGURE 4.20. STRESS PARAMETER AT LOCATION 5 FOR $\rho_s A_s / \rho_p bt = 3$

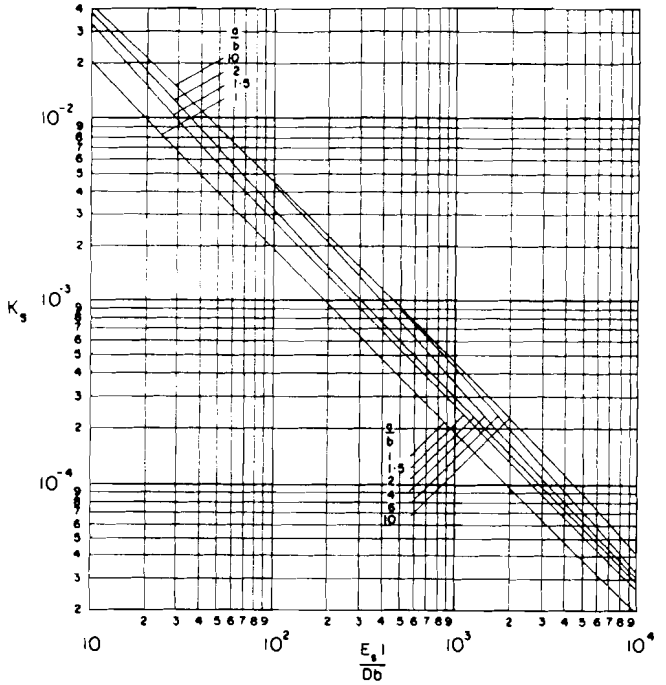

FIGURE 4.21. STRESS PARAMETER AT LOCATION S FOR $\rho_s A_s / \rho_p bt = 0$

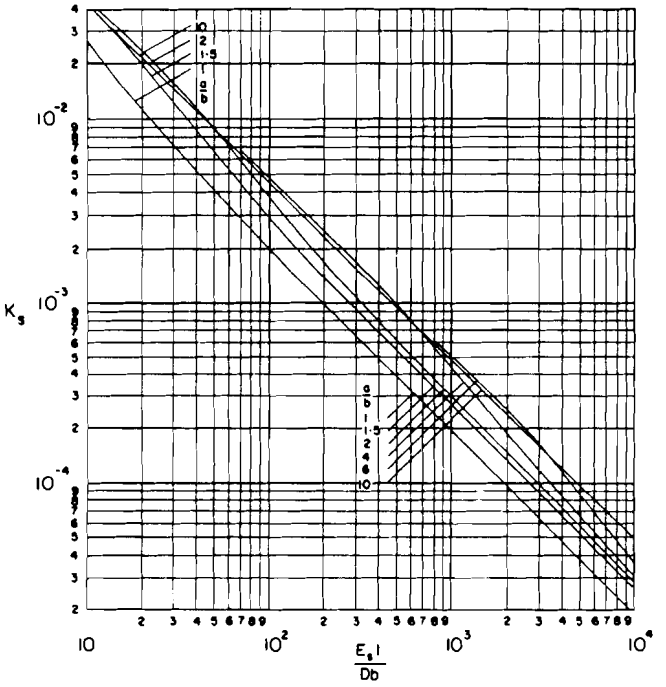

FIGURE 4.22. STRESS PARAMETER AT LOCATION S FOR $\rho_s A_s / \rho_p bt = 1$

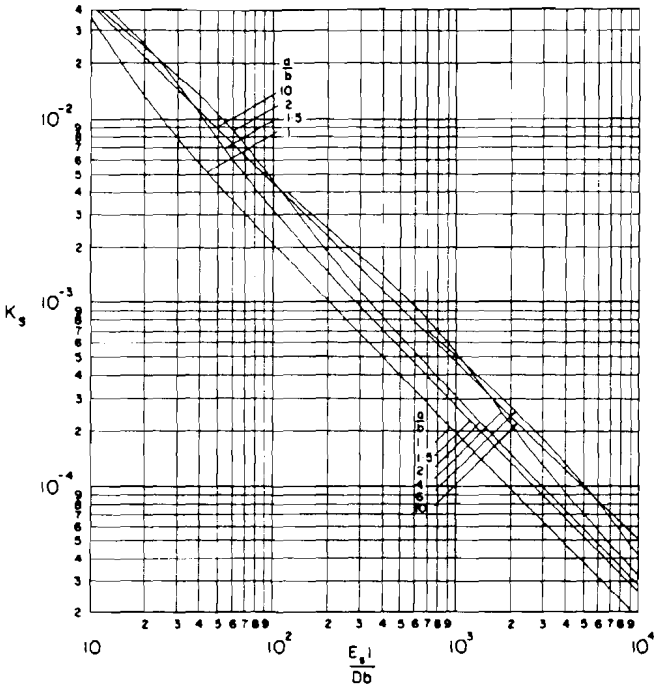

FIGURE 4.23. STRESS PARAMETER AT LOCATION S FOR $\rho_s A_s / \rho_p bt = 2$

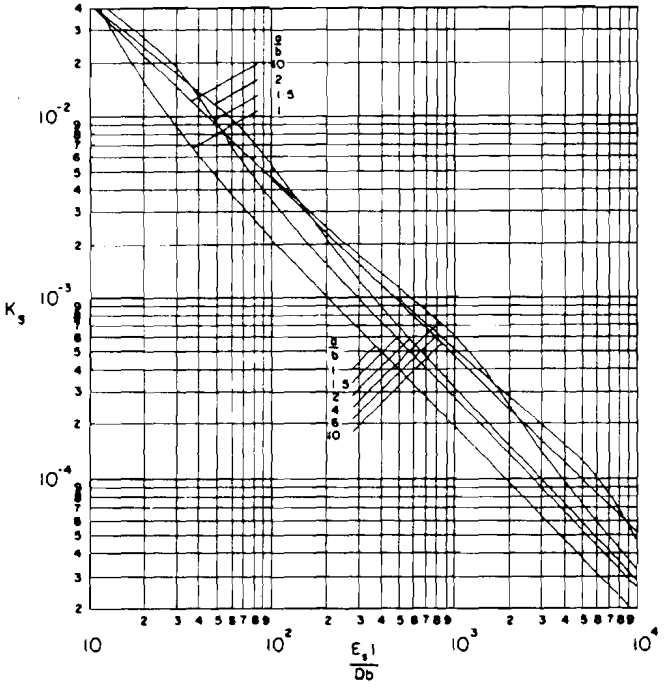

FIGURE 4.24. STRESS PARAMETER AT LOCATION S FOR $\rho_s A_s / \rho_p bt = 3$

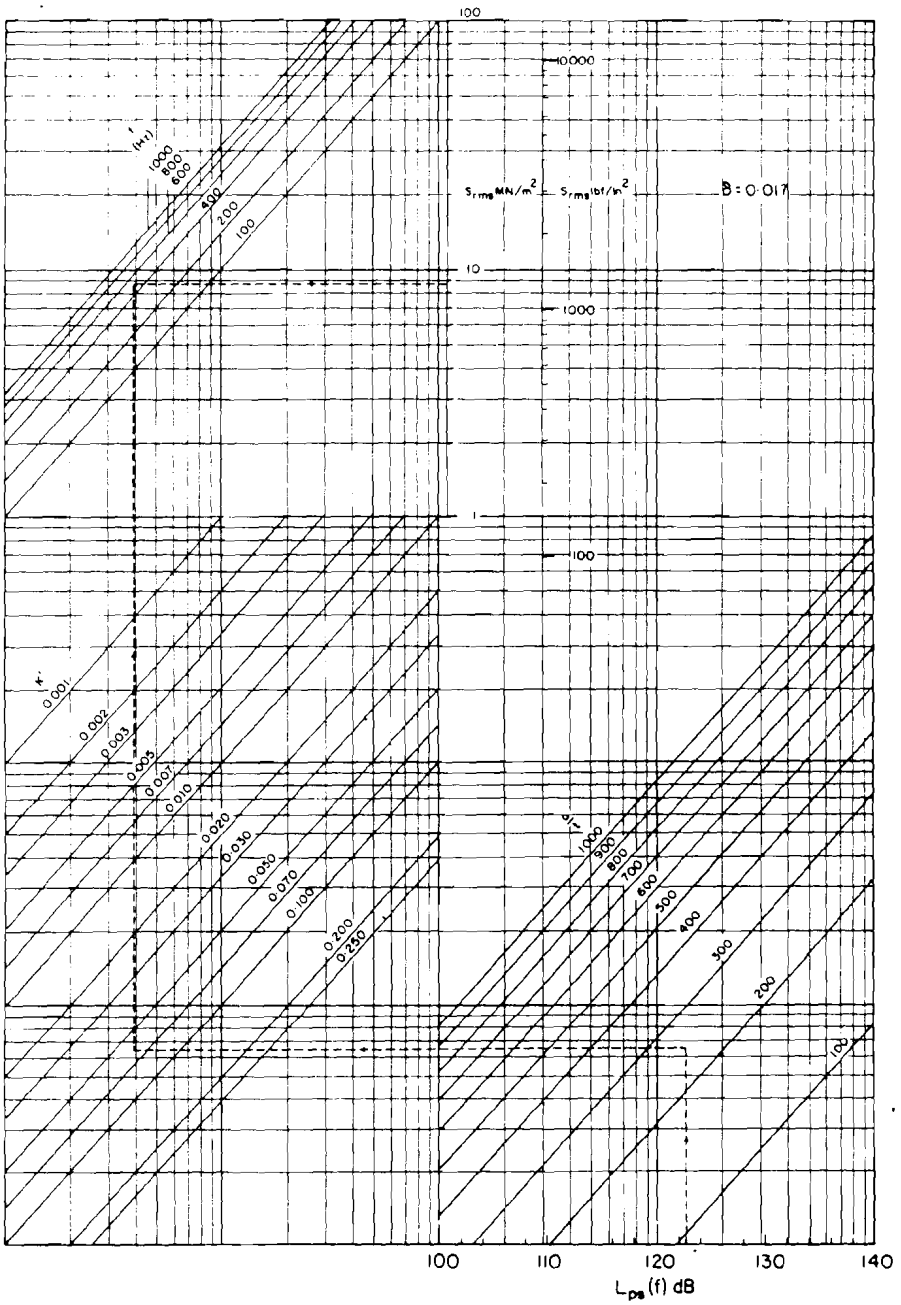

FIGURE 4.25. STRESS NOMOGRAPH

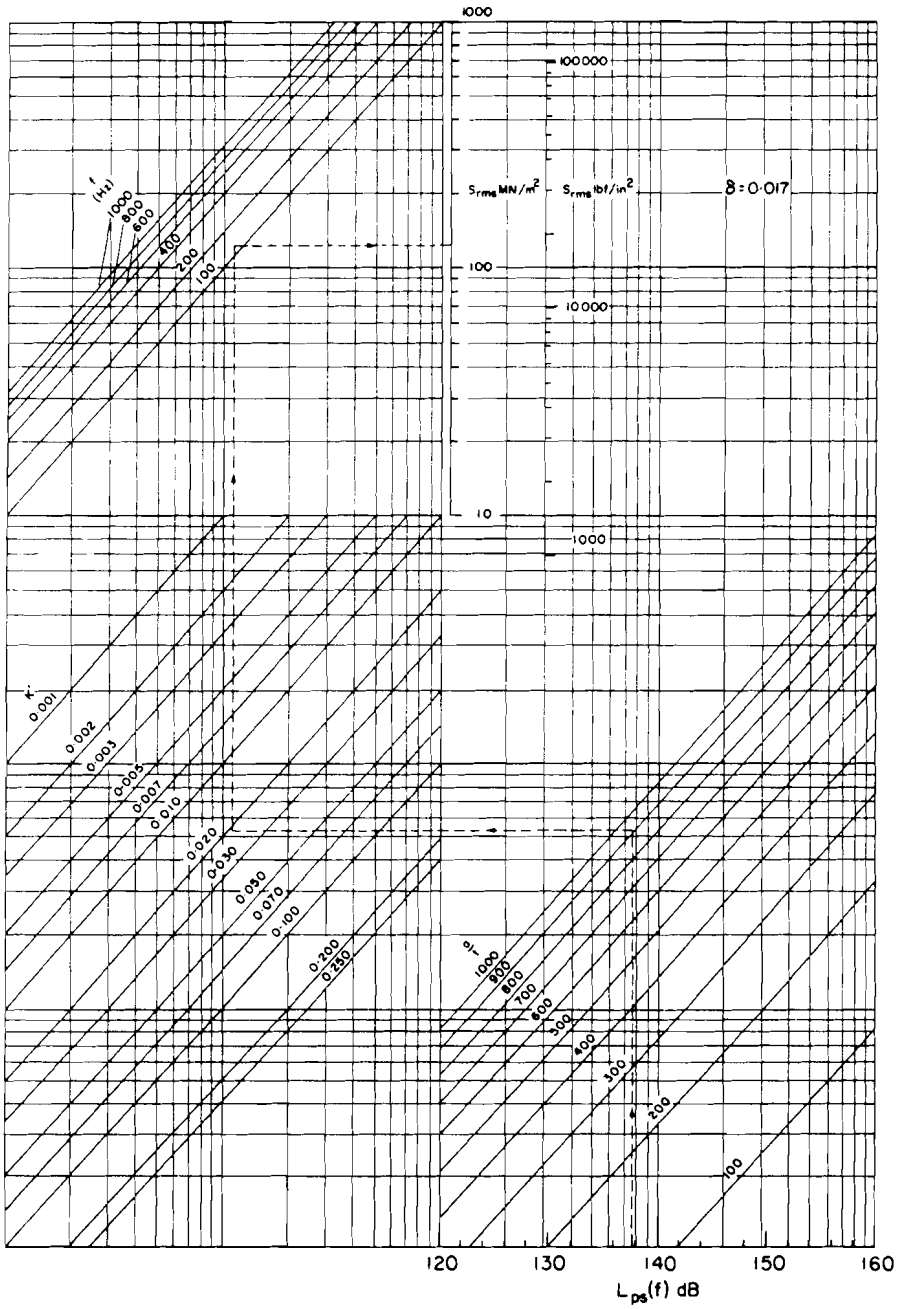

FIGURE 4.26. STRESS NOMOGRAPH

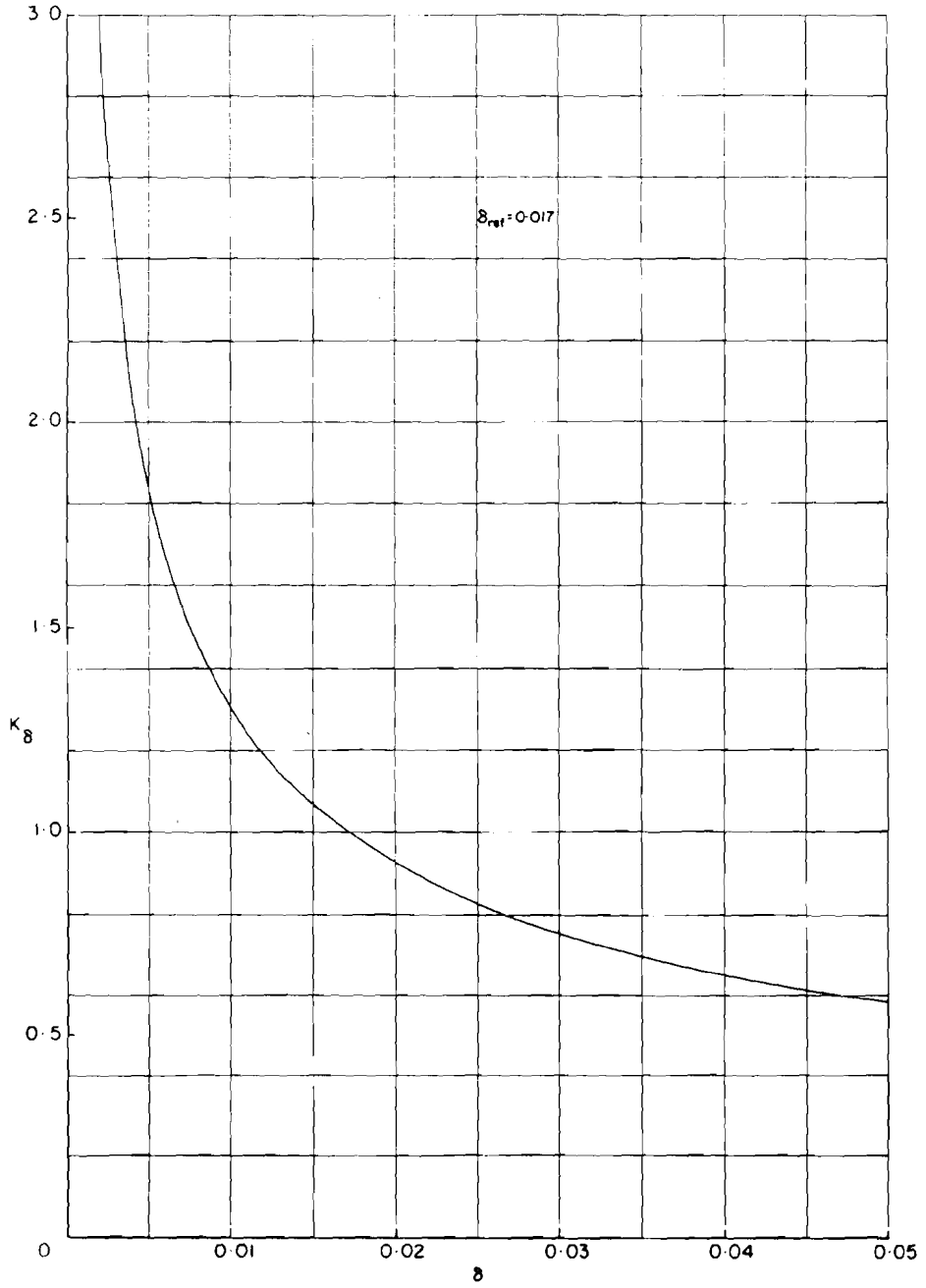

FIGURE 4.27. DAMPING RATIO CORRECTION FACTOR

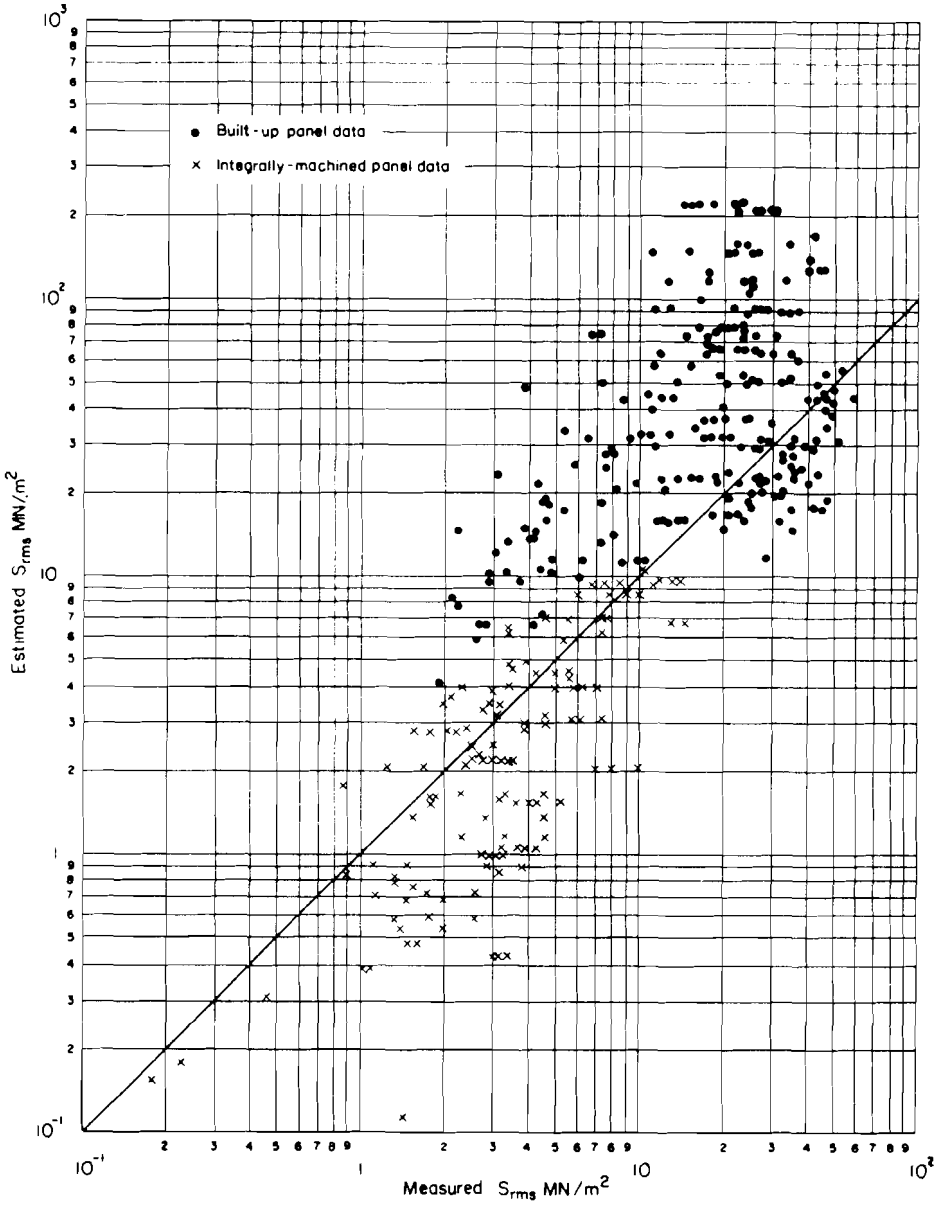

FIGURE 4.28. COMPARISON OF ESTIMATED AND MEASURED STRESS USING CALCULATED FREQUENCY AND $\delta = 0{\cdot}017$ FOR STRESS ESTIMATION

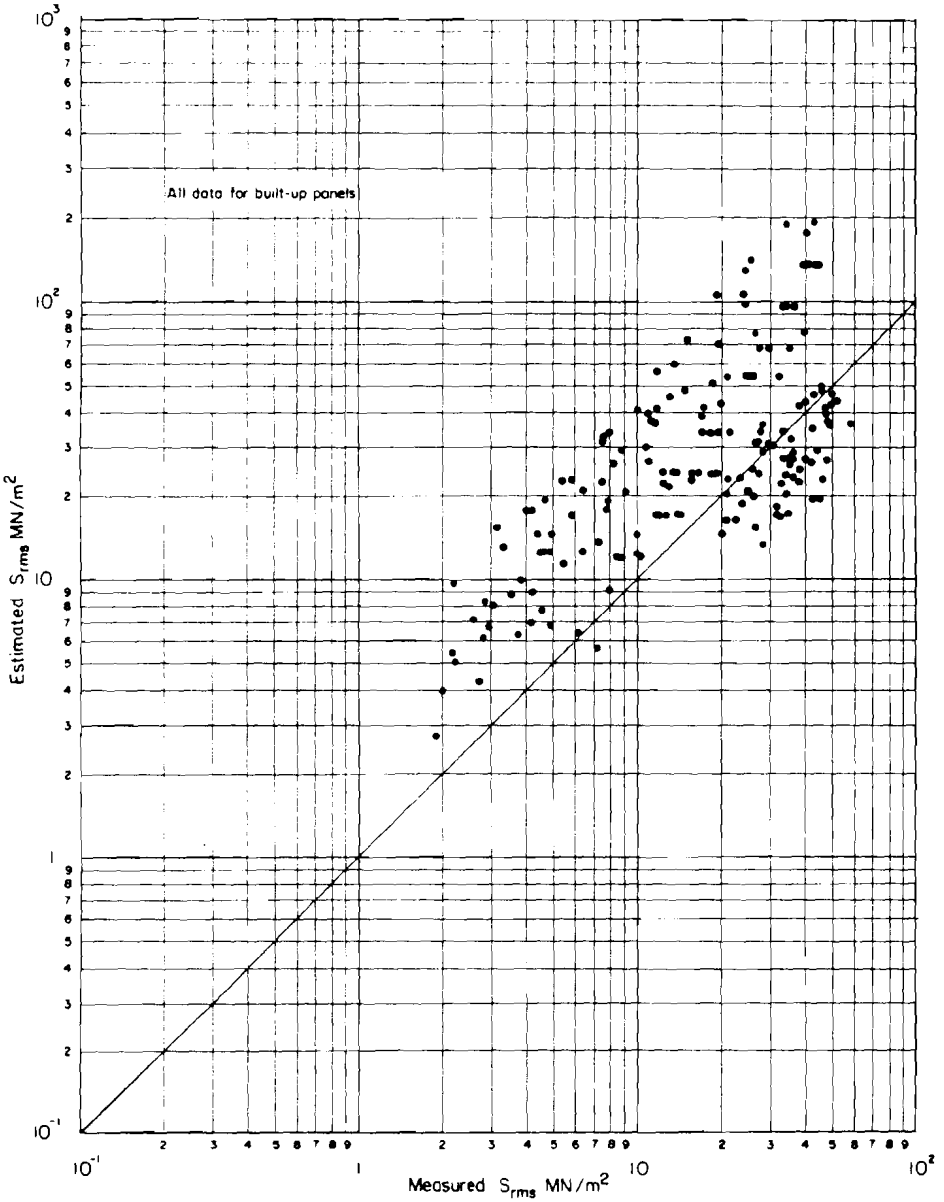

FIGURE 4.29 COMPARISON OF ESTIMATED AND MEASURED STRESS USING MEASURED FREQUENCY AND DAMPING RATIO FOR STRESS ESTIMATION

APPENDIX 4A

COMPUTER PROGRAM

4A.1 General Notes

The fundamental natural frequency and r.m.s. stresses of a panel with flexible stiffeners may be found using this computer program. The locations on the plate and stiffener at which r.m.s. stresses are estimated are given in Sketch (ii). The assumptions given in paragraph 4.2 are applicable to this program.

A listing of instructions for two sub-programs is given in FORTRAN IV programming language. A main program is required to read in data and print out calculated values of natural frequency and r.m.s. stress. A listing of instructions is not given for the main program as the instructions required are dependent on the particular computer used. The requirements for the main program are given below.

The main program must include the COMMON statement which is written in both the frequency and stress sub-programs.

4A.2 Frequency Sub-Program

This sub-program solves for the fundamental natural frequency of the plates. The plate edges are assumed to fixed against rotation.

The panel frequency data to be input for each panel considered are values for the variables listed in Table 4A.1.

TABLE 4A.1

Variable	Variable name	Variable	Variable name
A_s	AS	I	STI
a	A	t	T
b	B	ρ	RHO
E_p	EP	ρ_s	RHOS
E_s	ES		

Any coherent set of units in which time is expressed in seconds may be used, the frequency being obtained in Hz.

On returning to the main program from the frequency sub-program the fundamental natural frequency is stored in variable FREQ.

4A.3 Stress Sub-Program

This sub-program solves for the r.m.s. stress in the plate and stiffener. The geometric and physical property data required are the data for the frequency sub-program with the additional variable d in variable name DST. The panel stress data to be input for each stress case considered are values for the variables listed in Tables 4A.3.

TABLE 4A.3

Variable	Variable name
$L_{ps}(f)$	SPL
δ	DELTA

In this sub-program the r.m.s. fluctuating pressure equivalent to $L_{ps}(f)$ is computed. The units of this pressure in the sub-program are N/m^2. If British units are used this pressure must be calculated in units of lbf/in^2. To obtain this

pressure in British units the statement against label 106 should be replaced by

```
Y2=10.0**(SPL/20.0-8.53749)
```

On returning to the main program from the stress sub-program the r.m.s. stresses are stored in ARRAY STR as shown in Tabel 4A.4.

TABLE 4A.4

Stress location	1	2	3	4	5	S
Store location	STR(1)	STR(2)	STR(3)	STR(4)	STR(5)	STR(6)

SUBROUTINE FOR PANEL REFERENCE FREQUENCY

```
      SUBROUTINE FREQY
      COMMON AS,A,B,EP,ES,STI,T,RHO,RHOS,DST,SPL,DELTA,FREQ,STR(6),D,SK
      PNU=0.3
C
C CALCULATE PLATE REFERENCE FREQUENCY
C
      ALPHA=3.0*(A/B)**4+2.0*(A/B)**2
      D=EP*T**3/(12.0*(1.0-PNU**2))
      BETA=RHOS*AS/(RHO*B*T)-ES*STI/(D*B)
      GAMMA=ALPHA*(1.0+RHOS*AS/(RHO*B*T))+3.0*BETA
      X1=SQRT((GAMMA/(2.0*ALPHA))**2-2.0*BETA/ALPHA)
      X2=-GAMMA/(2.0*ALPHA)+X1
      X3=-GAMMA/(2.0*ALPHA)-X1
      X4=(X2*(ALPHA+3.0)+2.0)/(3.0*X2+2.0)
      X5=(X3*(ALPHA+3.0)+2.0)/(3.0*X3+2.0)
      IF(X5)100,100,101
  101 IF(X4-X5)100,100,102
  100 SKF=SQRT(X4)
      SK=X2
      GO TO 103
  102 SKF=SQRT(X5)
      SK=X3
  103 FREQ=6.2832*SKF*(SQRT(D/(3.0*A**4*RHO*T)))
      RETURN
      END
```

SUBROUTINE FOR PLATE AND STIFFENER R.M.S. STRESS

```
      SUBROUTINE STRESS
      COMMON AS,A,B,EP,ES,STI,T,RHO,RHOS,DST,SPL,DELTA,FREQ,STR(6),D,SK
      DIMENSION X(6)
      PNU=0.3
C
C CALCULATE RMS STRESSES
C
      Y=EP*T*A**2*(1.0+SK)/(19.7392*(1.0-PNU**2)*D*(SK**2*(3.0*(A/B)**4+
     12.0*(A/B)**2+3.0)+4.0*SK+2.0*(1.0+ES*STI/(D*B))))
      X(1)=2.0*SK*(A/B)**2-PNU
      X(2)=1.0-2.0*SK*(A/B)**2*PNU
      X(3)=1.0+2.0*SK
      X(4)=X(3)+2.0*PNU*SK*(A/B)**2
      X(5)=2.0*SK*(A/B)**2+PNU*(1.0+2.0*SK)
      X(6)=ES*DST*(1.0-PNU**2)/(EP*T)
      IF(DELTA)104,104,105
  104 DELTA=0.017
  105 Y1=(0.7854/DELTA)**0.5
  106 Y2=10.0**(SPL/20.0-4.69897)
      Y3=Y1*Y2*FREQ**0.5*Y
      DO 107 I=1,6
  107 STR(I)=Y3*ABS(X(I))
      RETURN
      END
```

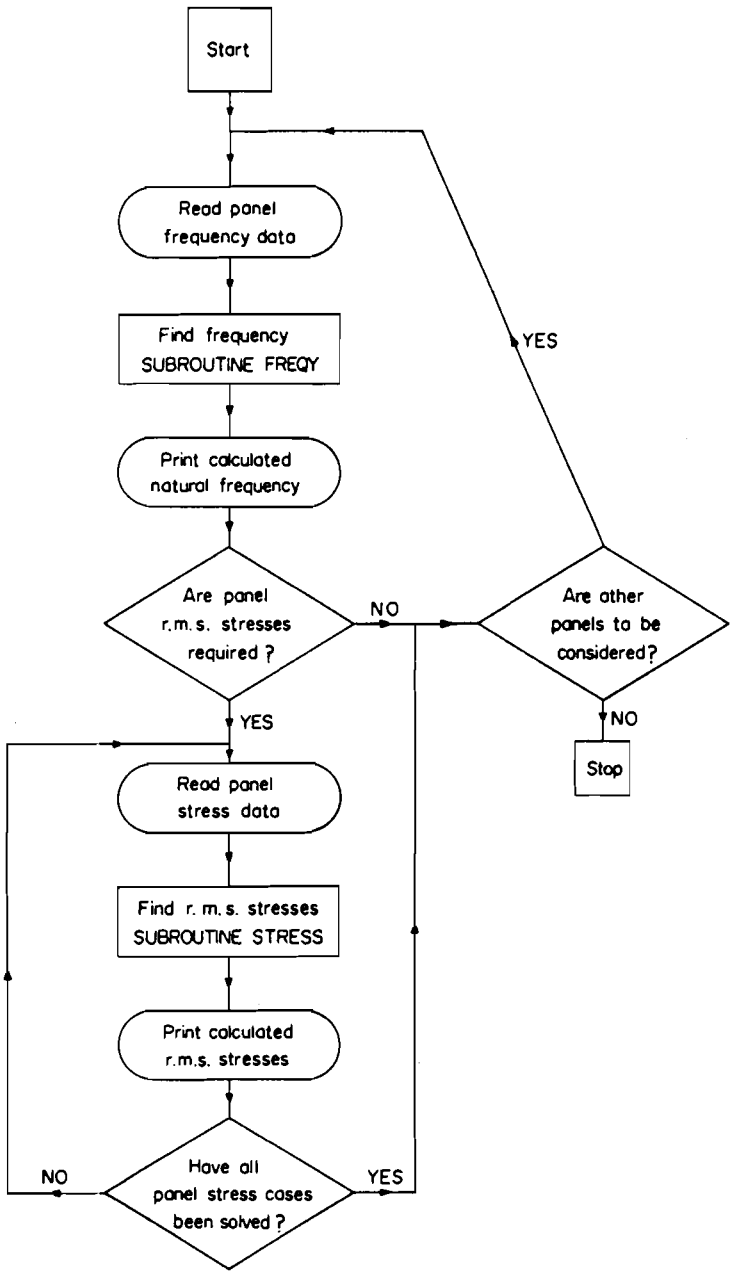

FIGURE 4 A.1 COMPUTER PROGRAM FLOW CHART

NATIONAL DISTRIBUTION CENTRES FOR UNCLASSIFIED AGARD PUBLICATIONS

Unclassified AGARD publications are distributed to NATO Member Nations through the unclassified National Distribution Centres listed below

BELGIUM
Coordonnateur AGARD – VSL
Etat-Major de la Force Aérienne
Caserne Prince Baudouin
Place Dailly, 1030 Bruxelles

CANADA
Director of Scientific Information Services
Defence Research Board
Department of National Defence – 'A' Building
Ottawa, Ont

DENMARK
Danish Defer
Østerbrogade
Copenhagen

FRANCE
O.N.E.R.A. (
29, Avenue
92, Cha lor

GERMANY
Bundes
Registra
53 Bonn
Postfach

GREECE
Hellenic Arr
D Branch, A

ICELAND
Director of
c/o Flugrad
Reykjavik

ITALY
Aeronautica Militare
Ufficio del Delegato Nazionale all'AGARD
3, Piazzale Adenauer
Roma/EUR

LUXEMBOURG
Obtainable through BELGIUM

NETHERLANDS
Netherlands Delegation to AGARD

National Aeronautics and Space Administration

WASHINGTON, D. C. 20546

OFFICIAL BUSINESS
Penalty For Private Use, $300.00
Special Fourth Class Mail

POSTAGE AND FEES PAID
NATIONAL AERONAUTICS AND
SPACE ADMINISTRATION

158 001 C4 B 07 740222 S00221EC
BOEING CO
VERTOL DIV
ATTN: LIBRARIAN, P32-01
P O BOX 16858
PHILADELPHIA PA 19142

nent

Orpington, Kent BR5 3RE

UNITED STATES
National Aeronautics and Space Administration (NASA)
Langley Field, Virginia 23365
Attn: Report Distribution and Storage Unit

* * *

If copies of the original publication are not available at these centres, the following may be purchased from:

Microfiche or Photocopy

National Technical
Information Service (NTIS)
5285 Port Royal Road
Springfield
Virginia 22151, USA

Microfiche

ESRO/ELDO Space
Documentation Service
European Space
Research Organization
114, Avenue Charles de Gaulle
92200, Neuilly sur Seine, France

Microfiche

Technology Reports
Centre (DTI)
Station Square House
St. Mary Cray
Orpington, Kent BR5 3RE
England

The request for microfiche or photocopy of an AGARD document should include the AGARD serial number, title, author or editor, and publication date. Requests to NTIS should include the NASA accession report number.

Full bibliographical references and abstracts of the newly issued AGARD publications are given in the following bi-monthly abstract journals with indexes:

Scientific and Technical Aerospace Reports (STAR)
published by NASA,
Scientific and Technical Information Facility,
P.O. Box 33, College Park,
Maryland 20740, USA

Government Reports Announcements (GRA),
published by the National Technical
Information Services, Springfield,
Virginia 22151, USA.

Printed by Technical Editing and Reproduction Ltd
Harford House, 7-9 Charlotte St, London. W1P 1HD